Numerical Study on Adhesively Bonded Stepped Joints

A Thesis

By

Md Sayed Anwar; BME1901017414

Md Mehedi Hasan Ziad; BME1901017494

Md Manirul Islam; BME1901017600

Md Ariful Hasan; BME1901017431

Supervised By

Md. Ahatashamul Haque Khan Shuvo

Assistant Professor

Department of Mechanical Engineering

Numerical Study on Adhesively Bonded Stepped Joints

Submitted to the
department of Mechanical Engineering
Sonargaon University (SU)
in partial fulfillment of the requirements for the award of the degree
of
Bachelor of Science in Mechanical Engineering

A Thesis

By

Md Sayed Anwar BME1901017414

Md Mehedi Hasan Ziad BME1901017494

Md Manirul Islam BME1901017600

Md Ariful Hasan BME1901017431

Supervisor: Md. Ahatashamul Haque Khan Shuvo

Assistant Professor

SONARGAON UNIVERSITY (SU)

Dhaka, Bangladesh

JANUARY 2023

ACKNOWLEDGMENTS

First and foremost, we would want to show our profound thankfulness to Almighty Allah for His bountiful blessings on our thesis work.

We would also want to convey cordial honor, respect, thankfulness to our honorable supervisor, **Md. Ahatashamul Haque Khan Shuvo**, Assistant Professor, Department of Mechanical Engineering, Sonargaon University for the guidance, helpful instructions, advices, and corrections during various stages of the thesis as well as, friendly cooperation throughout this thesis work.

We convey our honor and thankfulness to **Md. Mostafa Hossain**, Professor and Head, Department of Mechanical Engineering, Sonargaon University from our deep corner of heart for his support and encouragement.

We also want to convey sincere gratefulness to **Prof. Dr. Md. Abul Bashar**, Vice-chancellor of Sonargaon University.

We would specially thankfulness to **Dr. Md. Shariful Islam**, Professor, Department of Mechanical Engineering, KUET for his guidance and helpful instructions.

We would like to express our gratitude towards our parents and thank all faculty members and our classmate of the Department of Mechanical Engineering for their encouragement to perform the work. We also like to thank them, who helped us to complete this project successfully.

Authors

ABSTRACT

To investigate the behavior of different types of lap joints as material and geometric properties are varied under tensile loading, an analytically verified finite element parametric study was conducted on both ideally and adhesively bonded different types lap joints, measuring the changes in stress value at points of critical stress concentrations. Peel stresses increasing at the edges of the overlap area of the adhesively bonded single lap joints subjected to static tensile loading have an intense effect on the damage of the joint. In order to interrelate the finite element analysis with real-world lap joint behavior, digital image correlation was used to record the deformation of lap joint specimens under a tensile load. In this study, mechanical properties of the single lap joint (SLJ), one step lap joint (OSLJ) and three step lap joints (TSLJ) subjected to tensile loading were examined numerically by keeping the bonding area same for all six samples examined. As a result, it was observed that one-step lap geometry reduces the stress concentration increasing at the edges of the overlap area while the highest decrease occurred in the three-step lap geometry.

DECLARATION

We, hereby, declare that the work presented in this project is the outcome of the investigation and research performed by us under the supervision of Md. Ahatashamul Haque Khan Shuvo, Assistant Professor, Department of Mechanical Engineering, Sonargaon University (SU). We also declare that no part of this project and therefor has been or is or being submitted elsewhere for the award of any degree.

……. ……

MD SAYED ANWAR MD MANIRUL ISLAM

…….. ……

MD MEHEDI HASAN ZIAD MD ARIFUL HASAN

APPROVAL

This is to certify that the thesis on ‘‘**Numerical Study on Adhesively Bonded Stepped Joints’’** By (Md Sayed Anwar ID NO: BME1901017414, Md Mehedi Hasan Ziad ID NO: BME1901017494, Md Manirul Islam, ID NO: BME1901017600 Md Ariful Hasan ID NO: BME1901017431) has been carried out under my supervision. The project has been carried out in partial fulfillment of the requirements for the degree of Bachelor of Science (B.Sc.) in Mechanical Engineering of the year of 2023 and has been approved as to its style and contents.

……..

Md Ahatashamul Haque Khan Shuvo
Assistant Professor
Department of Mechanical Engineering

TABLE OF CONTENTS

LIST OF FIGURES

LIST OF TABLES

NOMENCLATURE

Symbol	Description	Unit
E	Young's modulus	MPa
G	Shear modulus	MPa
ν	Poisson's ratio	
σ_t	Ultimate tensile strength	MPa
ε_t	Ultimate tensile strain	mm/mm
E1, E2, E3	Modulus of elasticity in 1-, 2-, and 3-directions	MPa
G12, G23, G13	Shear modulus in the 1-2, 2-3, and 1-3 planes	MPa
σ_y	Peel stress	MPa
τ	Shear stress	MPa
F	Load	N
L	Overlap length	mm
ε1, ε2, ε3	Strain in 1-, 2-, and 3-directions	
C	Compliances	m/N
S	Stiffness	N/m

CHAPTER 1 INTRODUCTION

1.1 General:

Bonded composites have been used extensively in the aerospace and defense industries since the 1940s and 50s. Bonded composites are used in structures to strengthen slabs, beams, and columns. Other methods of retrofitting structures, such as steel jacketing of columns, have been around much longer in the field, but the use of composites has many advantages over other methods. Primarily, composites have a high strength-to-weight ratio, making them ideal for seismic retrofitting applications [1].

Adhesively bonded joints are preferred due to their advantages such as formation of uniform stress distributions, ability to join different materials, high fatigue resistance and impermeability [2].

However, in the adhesively bonded joints, extreme levels of stress concentration form at the edges of the overlap area, which significantly influences the strength of the joint. In order to use the adhesive bonding technique and to increase the load carrying capacity of the joint, the effect of these stresses forming at the free edges of the bonding area should be reduced. There are various types of the joints bonded with adhesives. The single-lap joint is the most commonly because of the simple geometry. This type of joint has been frequently used for joining composite materials [3,4,5].

There are many methods to increase the strength of the adhesively bonded joints by reducing the effect of these peeling stresses [6]. One of these methods is spew fille technique, which was shown to reduce the effect of these peeling stresses and increase the strength of the joint [7].

In the present study, mechanical properties of three different joints subjected to tensile loading having the same bonding area, namely, single lap joint (SLJ), one step lap joint (OSLJ) obtained by machining a single step and three step lap joints (TSLJ) obtained by machining three steps were studied numerically.

In the production of experimental samples, an aluminum alloy of AA2024-T3 was used as an adherent and flexible adhesive SBT9244 and stiff adhesive DP460 were employed as adhesives. After experimental studies on the three different joint types were conducted, stress analyses in the joints were performed with a three-dimensional finite element method by considering the geometrical non-linearity and the material non-linearities of the adhesive and adherent. Experimental studies were also performed in order to validate the results of finite element analysis [8].

In many engineering applications, advanced composite materials are used to fabricate many structural parts. This is due to their many characteristics such as light weight, high strength, high stiffness, good fatigue resistance and good corrosion resistance and to manufacture many complex geometries with fewer components [9].

Simulation may be defined as the imitation of the operation of a real-world process or system over time. In simulation any experiment or work is done computationally creation the same real-life atmosphere of that experiment. First the required model is developed with assigning its properties. It may be one part or assemble of some parts. Then the model is differentiated in several little pieces or meshed to run simulation. Here is a fact that the more the number of mesh, the accurate the result of the simulation. After meshing the model is then experimented numerically by some calculation by the given properties and situations and after that result comes. There are a few renowned software for simulation such as:

a) Ansys
b) NX
c) Autodesk CFD
d) Simulia Abaqus
e) MATLAB
f) Flexsim
g) Simulink etc.

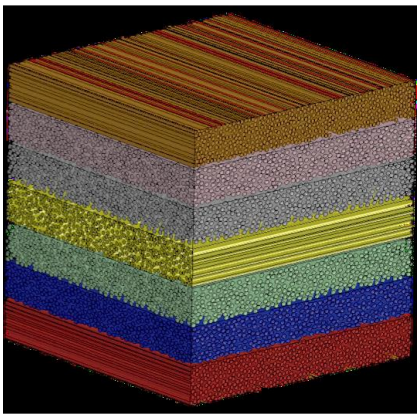

Figure 1.1: A typical composite material.

This work will first define lap joints and present an overview of several of the various lap joint geometries. Analytical derivation and verification are then presented, followed by a description and in-depth example of the parametric study conducted. The results are then presented, and discussed, followed by experimental work and validation, and both a conclusions and suggestions section.

1.2 Thesis organization:

In chapter 1, a general discussion about composite materials, its application in all sectors nowadays and the materials used for this thesis are provided. The thesis organization is given in this chapter. The objectives of this thesis are also outlined in this chapter.

In chapter 2, a comprehensive discussion about the composite materials and its classification is provided with different manufacturing techniques. A brief discussion on the different materials and adhesives for the construction of composite materials is also provided.

In chapter 3, Different types of the lap joints and different adhesive thickness are discussed. The setup of the numerical analysis and the working variables are also discussed in this chapter along with the analytical model of Displacement-Stress history for the verification of numerical model.

In chapter 4, the experimental results and discussion are included. Verification of the numerical model is also provided in this chapter.

In chapter 5, the conclusion of the study is provided stating the important findings and discussion about future work of this topics.

1.3 Objectives:

The objectives of this thesis are:

a) To study the stress distribution in a stepped joint with different number of steps.
b) To study the stress distribution with different adhesive thickness.

CHAPTER 2 LITERATURE REVIEW

2.1 Research Background:

Samples of three different joint types (Type-I, Type-II, and Type-III) used in the numerically studies were modeled three dimensionally by using Ansys package software [10]. The stress analyses in the adhesively bonded joints using a non-linear finite element method were performed by considering both the geometrical non-linearity and non-linear material behaviors of both adhesives (SBT9244 and DP460) and adherend (AA2024-T3). The dimensions of the samples and boundary conditions used in the finite element analyses were the same as those used in the experimental works.

In the 3D analysis, the adherend and adhesive of the adhesively bonded joint were modeled by using Abaqus software. Apart from this, smaller meshes were used in zones where the stress distribution is critical. The used material model is Multilinear Isotropic Hardening- von Mises plasticity (MISO). Also, for stress analysis the von Mises yield criterion was used to calculate the equivalent stress (req) and strain (eq) distributions in the adhesive layers and adherends. In addition, analyzing this model different mesh densities are used and the result of using many meshes is seen to be not very different, so in the paper due to both stress analysis and decreasing the duration of numeric solutions using this density of meshes is chosen.

2.2 Composite material:

Composite material is one of the most important fields in modern engineering because of its outstanding physical properties. From the ancient times to the modern era, it is being used. For example, in ancient times bricks were made up of clay and straw following this principle. Mixing of straw and mud to make wall of houses and huts is still used today in villages in Bangladesh. In modern technology the concept of composite material is not simply limited within mixing two components. Composites are being heavily used in numerous fields of engineering i.e., aeronautics, wind turbines, automobiles, electronics etc. [11].

Bonded composites have been in use for decades. During the second World War, the United States military began using glass fiber reinforced polymer composite vehicles in order to make the vehicles lighter and save steel [12] After World War II, the use of composites expanded into

markets outside of the military. Beginning in the 1950's, composite materials experienced widespread use in the aerospace industry. Fiber reinforced polymers (FRP) were utilized to produce airplane and rocket components and motor casings. In addition to the aerospace industry, composites are used in the automotive, marine, offshore drilling, sporting equipment, and civil engineering industries. Within the civil engineering field, composite materials are often used to strengthen and retrofit reinforced concrete slabs, beams, and columns.

A composite material is a material made from two or more constituent materials with significantly different physical or chemical properties that, when combined, produce a material with characteristics different from the individual components. The individual components remain separate and distinct within the finished structure.

Most recently researchers have also begun to actively include sensing, actuation, computation, and communication into composites which are known as robotic materials.

Typical engineered composite materials include:

- Mortars, concrete.
- Reinforced plastics such as fiber- reinforced polymer.
- Metal composites.
- Ceramic composites.

Composite materials are generally used for buildings, bridges, and structures such as tanks, imitation granite, cultured marble sinks etc. [13].

There are five basic types of composite materials: Fiber, particle, flake, laminar or layered and filled composites [14]

2.3 Adhesive Bonding:

Adhesive and Adhesion:

An adhesive is a substance which can hold materials together in a useful fashion by means of surface attraction. Surface attraction results from placing a thin layer of adhesive between two objects. An Adherend is the solid material in the adhesive joint other than the adhesive (also referred to as substrate). The bond line is the space or gap between two substrates which contains the adhesive. Adhesion is the process by which two surfaces are held together by interfacial forces (surface attraction) or mechanical interlocking. When an adhesive cures, it is converted from a

liquid to a solid state. This may be accomplished by cooling, loss of solvents or internal chemical reaction. Curing generally implies some type of physical or chemical change in the adhesive, while hardening or melting is reversible.

2.4 Adhesive Characteristics Required for Design and Analysis:

At the macro level, at which most bonded joint analyses are made, the mechanical data needed are complete stress–strain curves in shear for a range in temperatures covering the operating environment. Typical structural adhesives are stronger and more brittle at low temperatures and weaker and more ductile at high temperatures than at room temperature, as shown in Fig. Despite these great differences in bulk individual mechanical properties, the strength of structural joints (in which the adhesive strains are far from uniform) is far less sensitive to the test temperature than that of short-overlap test coupons (in which the adhesive strains are close to uniform, which is why they are used to generate the stress–strain curves). (This is explained in more detail below, in terms of elastic-plastic adhesive models [15]).

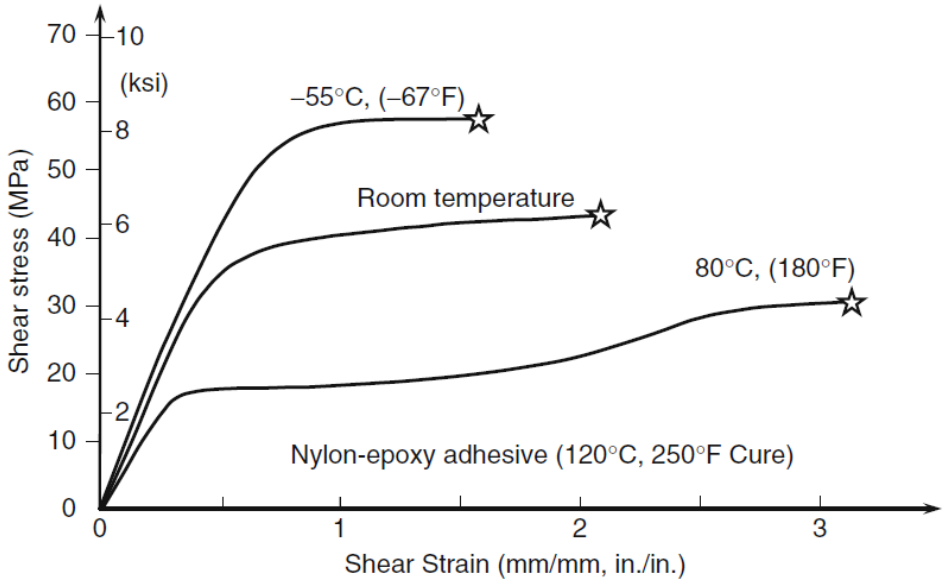

Figure 2.1: Adhesive stress–strain curves in shear, as a function of temperature.

This had its foundation in earlier such analyses developed by Gosse [16] for the failure of homogeneous polymers, including adhesives constrained between much stiffer adherends. There

are only two possible failure mechanisms available for any solid homogeneous material. One is dilatation which, in the context of adhesively bonded joints, is associated with the induced peel stresses at the ends of the bonded overlap. The other is distortion, which is the dominant behavior of the adhesive layer away from the ends. The value of the first strain invariant, the sum of three orthogonal strain components,

$$J_1 = \varepsilon_1 + \varepsilon_2 + \varepsilon_3 \qquad ( )$$

cannot be measured on any pure (neat) adhesive test coupon because failure by distortion according to the other (von Mises shear strain) invariant

$$\gamma VMcrit = \sqrt{\frac{1}{2}[\,(\varepsilon' - \varepsilon')^2 + (\varepsilon' - \varepsilon')^2 + (\varepsilon' - \varepsilon')^2]}$$

(Where the prime denotes principal values) occurs before the dilatational limit had been reached. Failure of polymers by dilatation (increase in volume) occurs only in a constrained environment, as between two circular rods bonded at their ends and pulled apart, as in (or between the adherends in bonded joints).

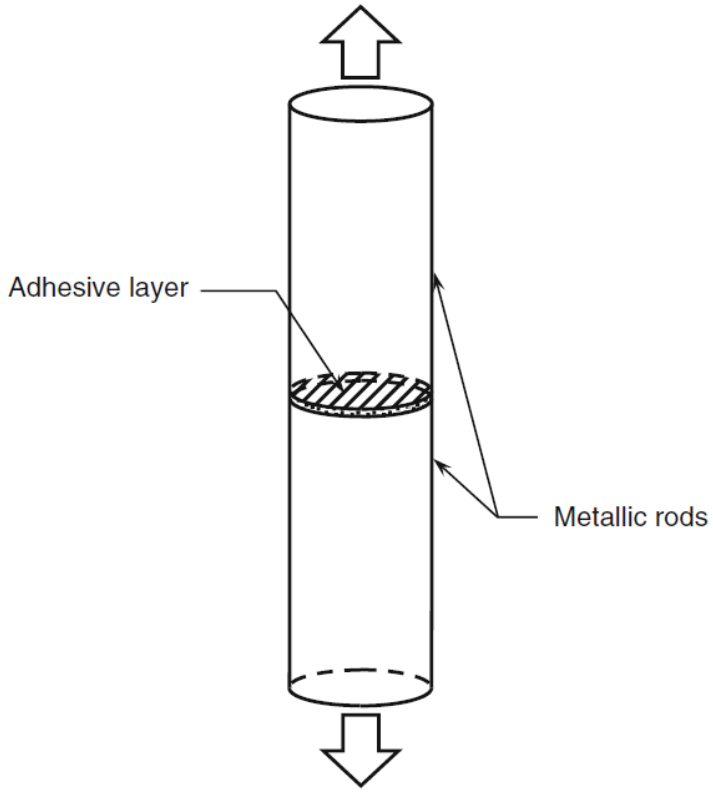

Figure 2.2: Butt-jointed test coupon to measure J1 strain invariant for adhesives.

2.5 Design of Adhesively Bonded Joints:

The design and analysis procedures cited under three government-sponsored R&D contracts over a period of years. The first was for NASA Langley during the period 1970–1973 in which the elastic-plastic adhesive model was introduced and the first of the A4E…. series of Fortran computer codes was derived. The second increment of work was for the USAF at WPAFB, during and following the PABST bonded fuselage contract, from 1976 through 1983. Three new computer codes, A4EI, A4EJ, and A4EK, were produced and the effects of flaws and variable bond layers were covered [17].

The design of double-lap and single-lap bonded joints between nominally uniformly thick adherends is straightforward. The design of the 100% full-load transfer bonded joints with no failsafe rivets for the pressurized PABST bonded fuselage, [18] was reduced to a single table of overlap versus skin thickness, supplemented by a requirement to gently taper the ends of the overlaps locally for the thicker skins to prevent premature-induced peel failures. It is crucial to note that the overlaps are universal in the sense that they are independent of the magnitude of any applied loads. This enables the design of the bonded joints to be completed before the internal loads in a structure have been established. The key to this design method is explained in Fig.

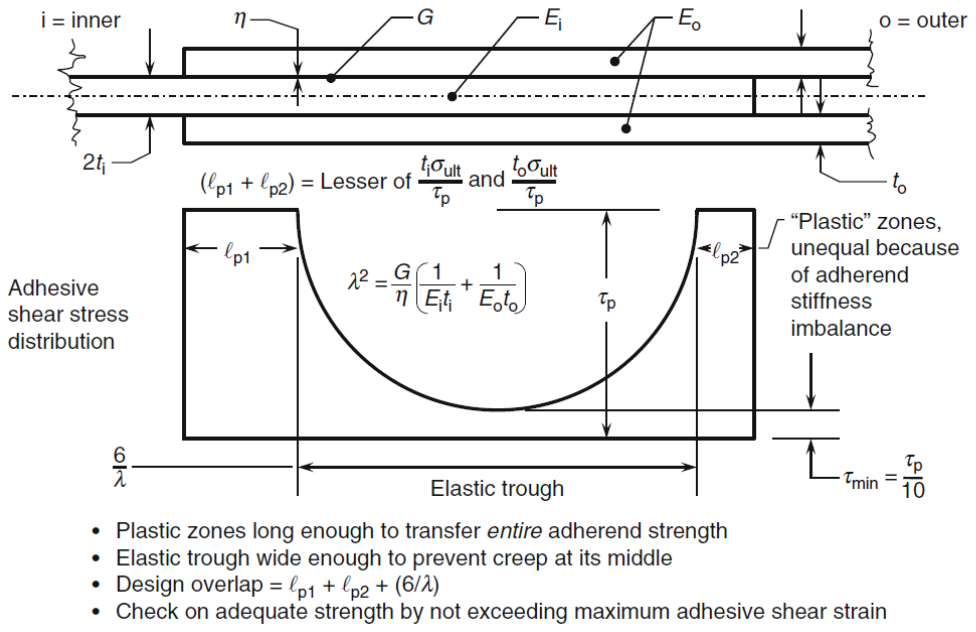

Figure 2.3: Design of Adhesively bonded joints.

2.6 Different type of Joints:

2.6.1 Scarf joint:

A scarf joint (also known as a scarph joint) is a method of joining two members end to end in metalworking The scarf joint is used when the material being joined is not available in the length required.

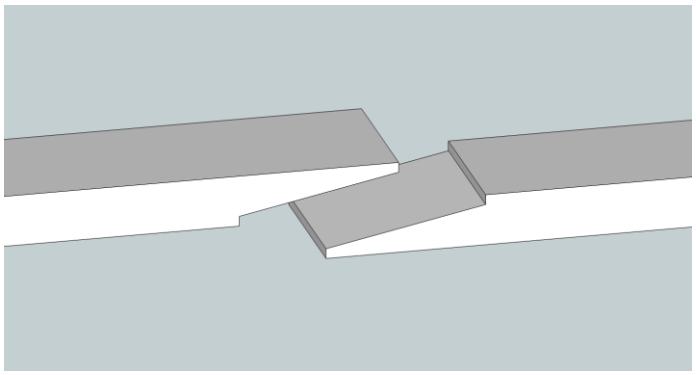

Figure 2.4: Scarf joint.

2.6.2 Double Scarf joint:

A scarf joint, or scarph joint, is used to join two pieces of wood or metal end to end. It is a simple form of a lap joint, and when the two pieces are joined together, produces a virtually invisible seam.

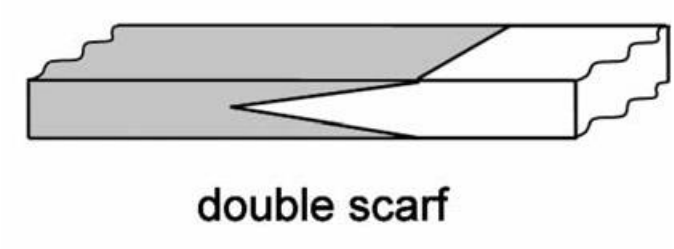

Figure 2.5: Double scarf.

2.6.3 Butt joint:

A butt joint is a technique in which two pieces of material are joined by simply placing their ends together without any special shaping.

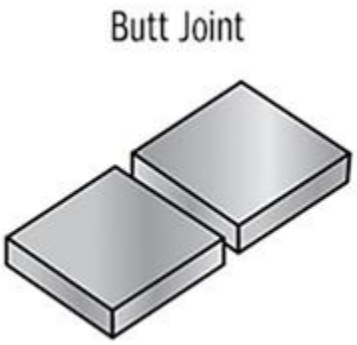

Figure 2.6: Butt Joint.

2.6.4 Lap joint:

A lap joint or overlap joint is a joint in which the members overlap. Lap joints can be used to join wood, plastic, or metal. A lap joint can be used in woodworking for joining wood together.

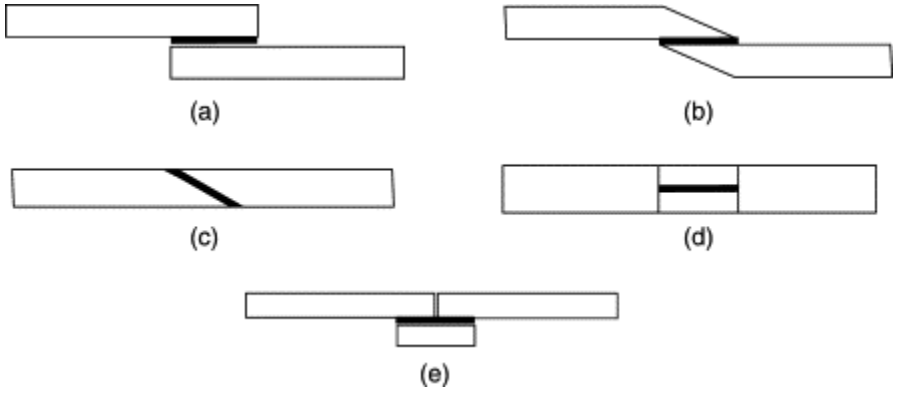

Figure 2.7: Lap joint.

2.6.5 Single-lap Joints:

Single-lap joints are created using an adhesive layer to connect two adherends. Figure 2.8 shows a typical single-lap joint. Adhesive bonding is an alternative to mechanical bonding that avoids the use of drilled holes and reduces stress concentrations. However, stress concentrations do still exist at the end of each adherend. The two types of stresses occurring in an adhesively bonded joint are transverse normal tensile (peel) stress and shear stress.

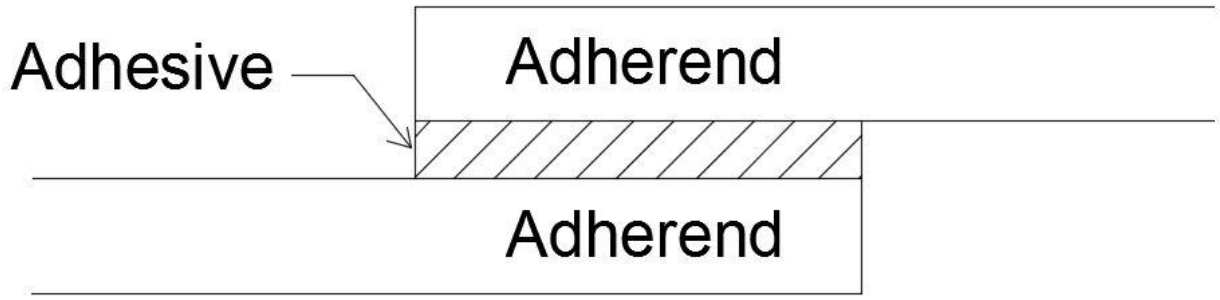

Figure 2.8: Single-lap joint geometry

Due to a sudden change in stiffness, stress concentrations occur at the lap location with the maximum stresses occurring at the overlap ends [**Error! Reference source not found.**]. If a spew fillet is present at the ends of the adherends, the maximum adhesive stresses have been shown to be much lower than if the ends are squared off as they are in Figure 1 [19]. Figure 2 shows an example of a single-lap joint with a spew fillet on the adherend ends.

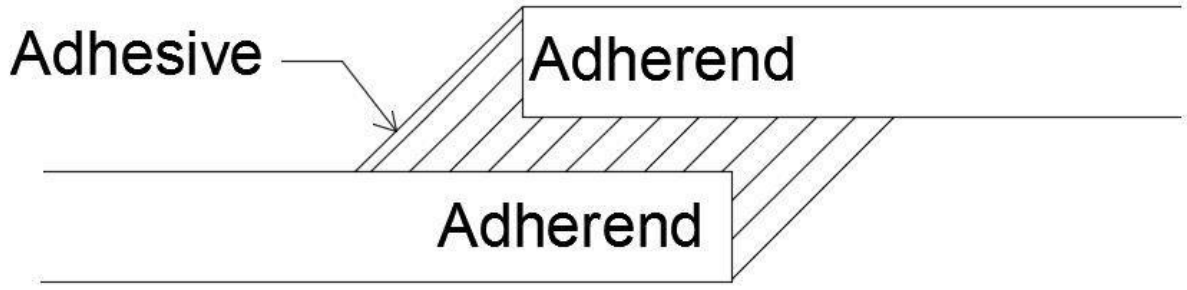

Figure 2.9: Single-lap joint with spew fillet.

2.6.6 Double Lap Joint:

double lap joint is a balanced construction configuration joint that consists of two outer adherends that are bonded on both sides of center (inner) adherend

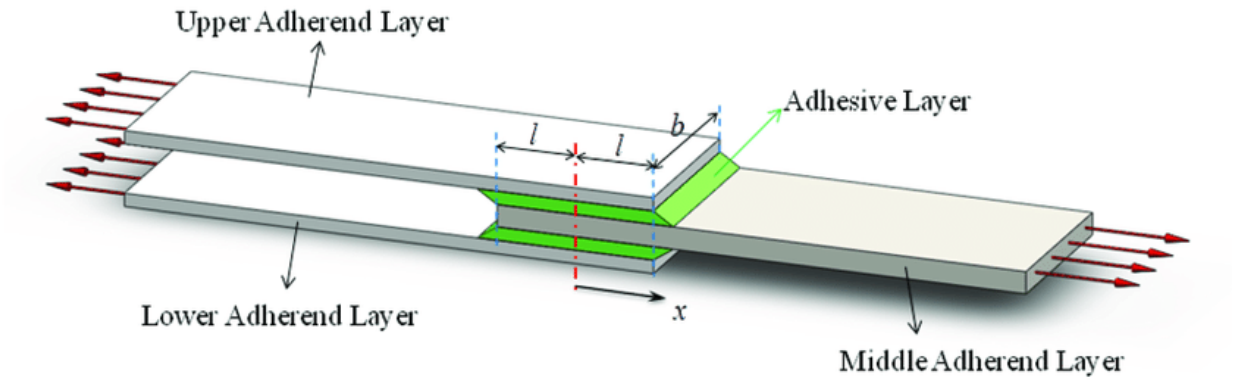

Figure 2.10: Double lap joint.

2.6.7 Stepped Joint:

The step-lap joint is essentially a series of overlap joints and is an outline of the simple one-dimensional and three-dimensional analytical model. with the overlap joint, the stepped-lap joint has a non-uniform shear stress distribution with high stresses at the ends of each step. With correct design, the step-lap joint can join adherends of any thickness.

2.6.8 One Step Lap Joint:

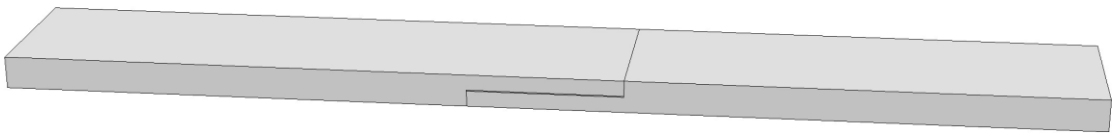

Figure 2.11: One-step lap joint.

2.6.9 Three Step Lap Joint:

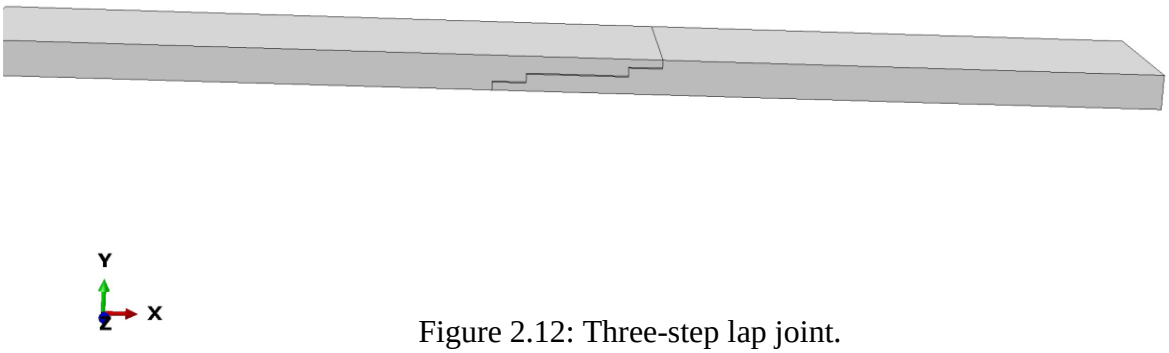

Figure 2.12: Three-step lap joint.

2.7 Design Features Ensuring Durability of Bonded Joints:

Durability in bonded joints requires both that the bonded interfaces are stable (the glue stays stuck) and that the adhesive is not failed by the combination of mechanical loads and residual thermal stresses caused by dissimilar adherends. The first issue has nothing to do with the geometry of any bonded joint, although joints fail faster under peel-dominated loads than under shear loads. This is the little understood requirement represented by setting the minimum stress level at or less than 10% of the maximum, which defines the overlap needed to prevent any creep from accumulating. The need for such a requirement was exposed by some of the early fatigue tests on the PABST program. Quite misleading conclusions, both positive and negative, could be drawn from durability tests on short-overlap coupons, [20] The key to the success of these designs was the acknowledgement that the adhesives shear stresses were, and should be, highly nonuniform.

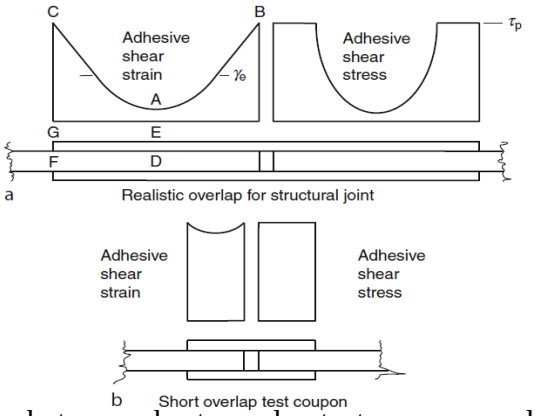

Figure 2.13: Differences between short-overlap test coupons and long-overlap bonded joints. (a) Realistic overlap for structural joint. (b) Short-overlap test coupon.

The reason why properly designed bonded joints do not suffer from mechanical fatigue failures is that the most critical conditions are not developed where the adhesive is protected by the adherends. This can be understood by characterizing the minimum and maximum adhesive shear strains as a function first of bonded overlap and secondly as a function of adherend thickness, accounting for the effect of the environment in each case. This is illustrated in Fig, for room temperature.

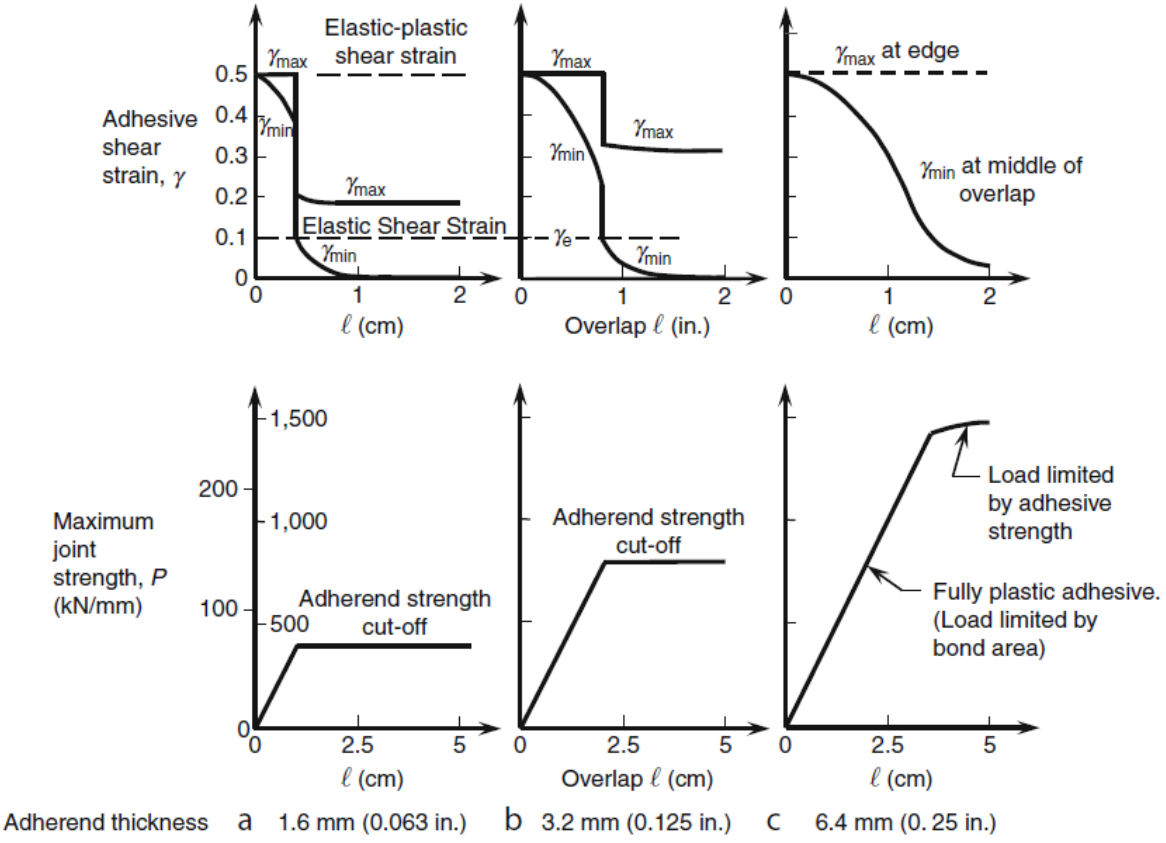

Figure 2.14: Effects of adherend overlap and thickness on maximum and minimum shear strains at room temperature.

2.8 Effects of Thermal Mismatch Between Adherends on Strength of Bonded Joints:

When thermally dissimilar materials are bonded together, residual thermal stresses are developed that usually detract the remaining strength available for transmitting mechanical loads. These phenomena occur whenever titanium edge members are bonded around the edges of composite panels to permit the use of mechanical fasteners during final assembly of the structure or to permit disassembly in service for inspections and repairs. These thermal stresses

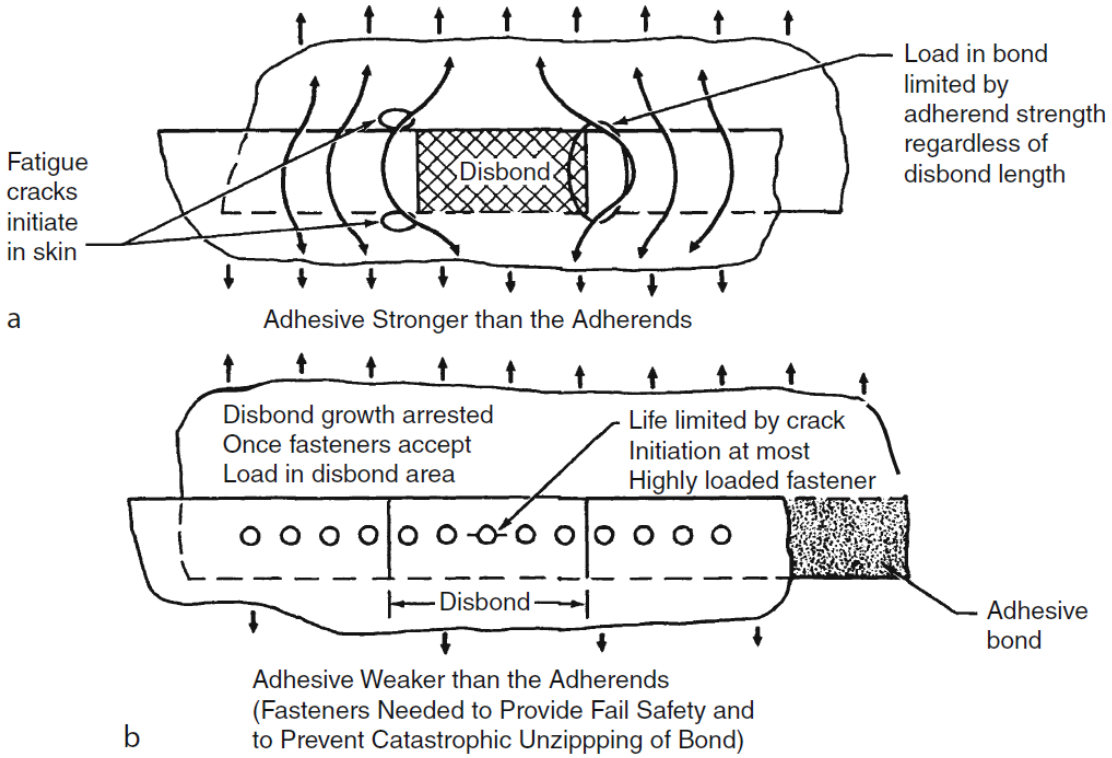

Figure 2.15: Two-dimensional load redistribution around a large flaw in a bonded overlap: (a) Adhesive stronger than the adherends; (b) Adhesive weaker than the adherends.

are roughly proportional to the difference in temperature between the curing and operational temperatures. Their analysis is explained by [22] and illustrated in Fig. load cases for most space structures.

2.9 Types of Adhesives:

Modern adhesives are classified either by the way they are used or by their chemical type. The strongest adhesives solidify by a chemical reaction. Less strong types harden by some physical change. Key types in today's industrial scene are as follows [23].

- Anaerobic
- Cyanoacrylates
- Toughened Acrylics/ Methacrylate
- UV curable adhesives
- Epoxies
- Polyurethanes

- Modified Phenolics

The above types set by chemical reactions. Types that are less strong, but important industrially, are as follows:

- Hot Melts
- Plastisol
- Rubber adhesives
- Polyvinyl Acetates (PVAs)
- Pressure-sensitive adhesives

2.10 Failure Modes:

a general classification is created and failure types are collected in 3 main groups which are explained in more detail in the following sections.

2.10.1 Cohesive Failure:

The cohesive failure represents the failure within the adhesive bulk material (Figure 2.16) which is the most desirable mode of failure. It takes place where peel stress or out of plane stress increases. As a matter of fact, they cause joint eccentricity and large deformations in adherends. The joint eccentricity causes cohesive failure because adhesives are known to be weak in the out of plane direction [24].

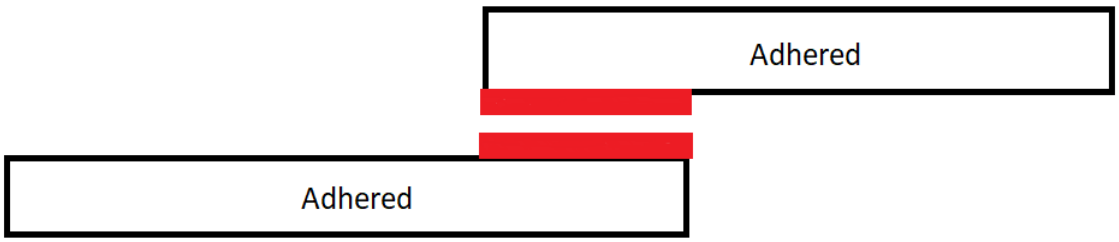

(A)

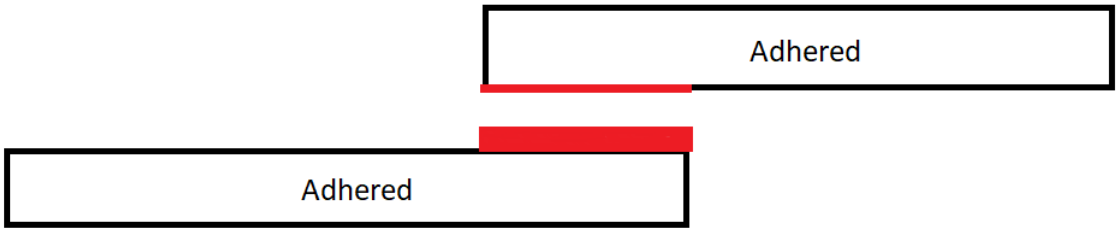

(B)

Figure 2.16: Cohesive Failure of Bonded Lap Joint A and B

2.10.2 Adhesive Failure:

Adhesive failure would occur along the interface between the adhesive and adherend as shown in (Figure 2.17) General cause of this phenomenon is improper surface preparation.

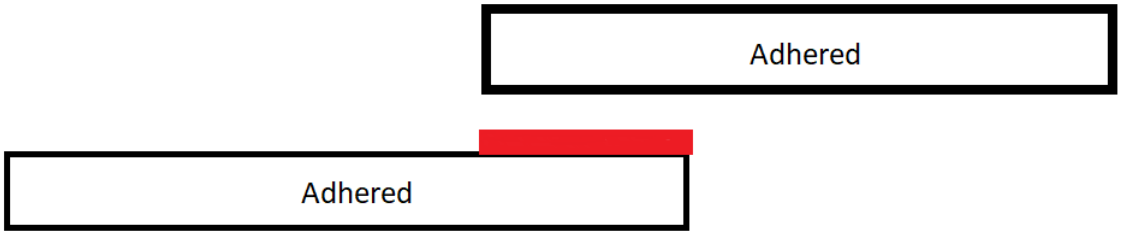

Figure 2.17: Adhesive Failure of Bonded Lap Joint.

2.10.3 Adherend Failure:

Failure within the FRP substrate is called as adherend failure. Adherend failure either occur with rupturing a piece of FRP substrate or rupture one of the adherend completely. The general cause of failure in adherends are high shear stresses at bonded joints since shear strengths of adhesives are relatively higher than laminates. Adherend failure representation is given in (Figure 2.18)

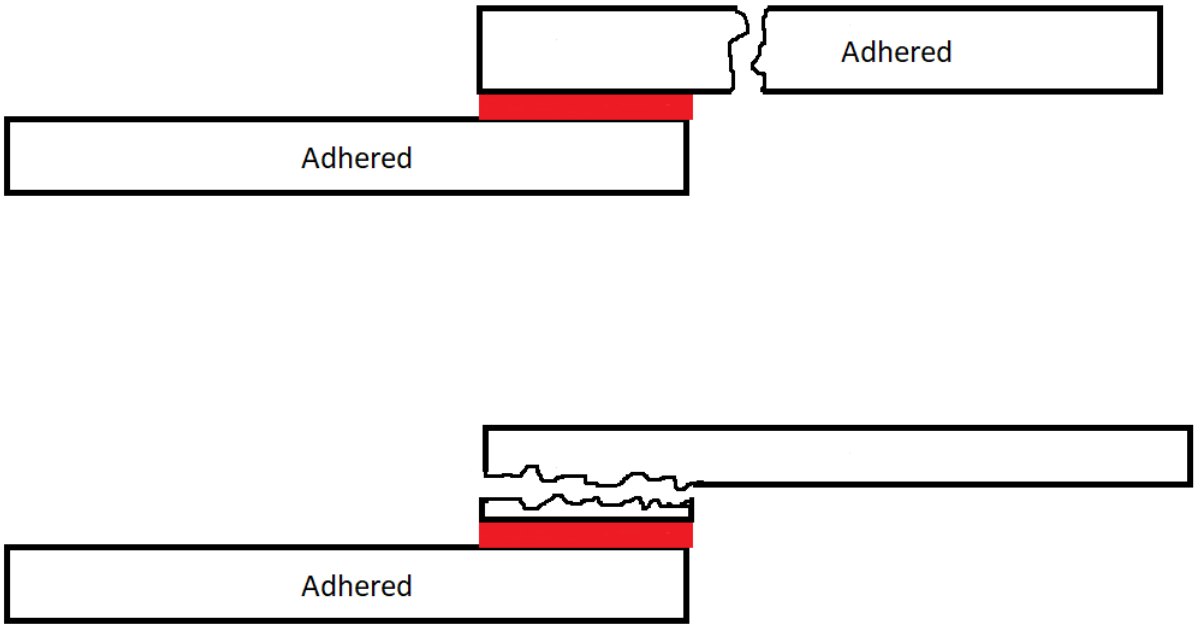

Figure 2.18: Adherend Failure of Bonded Lap Joint

2.11 Failure Analysis of Bonded Joints:

Reliable and efficient use of bonded joints is depending on the design and methodology can be costly. Finite element analysis plays an important role at this point to obtain optimum design of structures. By using finite element method, accurate predictions can be achieved for joint strength and failure behavior. There are mainly three approaches to perform failure analyses, which are continuum mechanics, fracture mechanics and damage mechanics.

2.11.1 Continuum Mechanics:

General concept in this approach is simply comparing the material allowable with the maximum stress and/or strain values as output of analyses. In continuum mechanics, materials are assumed to be continuous and there is no solution at the singularity points. Therefore, mesh refinement near the singularity points is highly determinative on the results of the analyses [25].

2.11.2 Fracture Mechanics:

In contrast to continuum mechanics, this approach is capable to derive a solution at crack tips. However, a pre-existing crack is required to be defined within this method. While crack initiation can be calculated with continuum mechanics, fracture mechanics is a favorable method to deal with crack propagation. Fracture mechanics uses the stress intensity factor (K) to determine the stress state at singularity points like a crack tip [26]. Failure mechanism works when the stress intensity factor reaches the fracture toughness of the material. Fracture toughness represents the critical fracture energy (Gc). Fracture mechanics principle differs depending on the loading on the crack tip as shown in Figure. There are three modes of loading;

- Mode I; opening mode
- Mode II; in-plane shear mode
- Mode III; out-of-plane shear mode

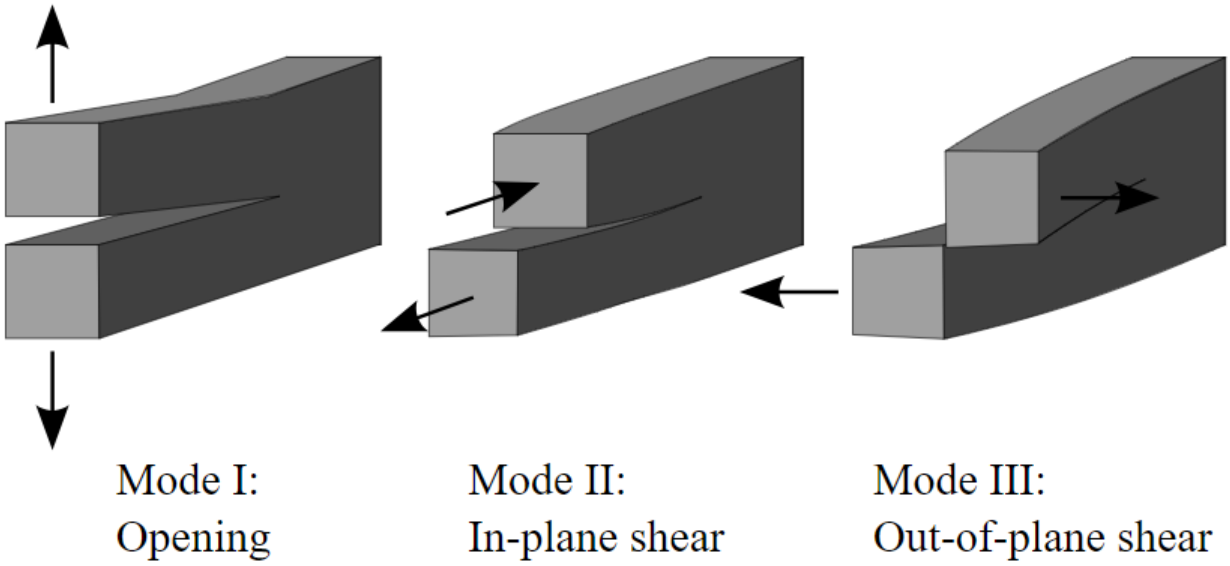

Figure 2.19: Adherend Failure of Bonded Lap Joint

2.11.3 Damage Mechanics:

Damage mechanics is a method to predict both initiation and propagation in the structure until the complete structural failure. It can be divided into two main parts, which are local approach and continuum approach. The local approach is used to predict the interfacial failure between two surfaces. Interface elements are modelled with zero volume line. While continuum approach uses

finite thickness elements to simulate failure of the bulk material (adhesive). Between these two approaches a specified model is categorized that is called as the cohesive zone model (CZM). CZM is used for the paths defined in local and continuum approaches and combine the response of traction-separation to simulate crack initiation and propagation. In the following chapter, a detailed information and methodology of cohesive zone model is given. [27]

2.12 Advantages of Adhesive Bonding:

- The bond is continuous
- Stiffer structures
- Improved appearance
- Complex assemblies
- Dissimilar materials
- Reduced corrosion
- Electrically insulating
- Reduced stress concentrations
- Jointing sensitive materials
- Vibration damping
- Simplicity

All these advantages may be translated into economic advantages: improved design, easier assembly, lighter weight (inertia overcome at low energy expenditure), longer life in service.

2.13 Disadvantages of Adhesive Bonding:

- Requires careful substrate (adherent) surface preparation;
- Long mixing and curing time may be required;
- Importance of right joint design;
- Difficult disassembly of joined parts;
- Necessity to fixture (hold together) the joined parts during curing;
- Service temperature and environment limitation;
- Low creep strength;

- Changing properties during service

2.14 Application of Adhesive:

Adhesive resins are used as an adhesive layer in numerous applications which consist of multiple layers of barrier materials. Not only does the adhesive resin ensure that manufacturers meet environmental, regulatory and industry requirements but it also enhances adhesive performance and durability.

2.14.1 Automotive Applications:

- Plastic Fuel Tanks
- Fuel Lines
- Fuel Filler Pipes
- Fuel Connectors

2.14.2 Adhesives for the Aerospace industry:

Our aerospace adhesives include both flammable and non-flammable formulations that provide a strong, permanent, and robust bond even in the most demanding of environments, ensuring all relevant safety standards are met.

2.14.3 Packaging Applications:

Adhesive Resin for Cosmetic Packaging Applications:

- Body lotion containers
- Make up bottles
- Oval and round tubes

2.14.4 Adhesive Resin for Pharmaceutical Packaging Applications:

- Tubing
- PTP packaging
- Bottles

2.14.5 Adhesive Resin for Food Packaging Applications:

- Ketchup
- Salad dressing

- Pudding
- Meat and Soup
- Cheese
- Pasta and Apple sauce
- Beverages

2.14.6 Industrial Applications:

In industrial markets, epoxy resins as an adhesive ideal for several uses including floor heating pipe, aluminum sheathe and bottle applications. Also, the emerging use of these adhesives is in aerospace and automotive industries. These are used for floor and ceiling fixing, external body building and for interior designing of the compartments and dashboards. High temperature adhesives are employed in jet airplanes for sustaining high force and temperature developed at high speed and air resistance.

2.14.7 Oil and Gas Pipe Applications:

In the oil and gas sectors, pipeline bonding and coatings are expected to perform under severe conditions and extreme temperatures. These adhesive resins can be easily processed by co-extrusion with polypropylene or polyethylene with circular die for middle or small diameter steel pipes, and with flat die for larger diameter steel pipes.

2.15 Limitations of Adhesive Bonding:

- Temperature resistance
- Chemical resistance
- Curing time
- Process controls
- In service repair

CHAPTER 3 COMPUTATIONAL MODELING

3.1 General Equation:

Strain–stress relationship is

$$\varepsilon_i = S_{ij}\sigma_j, i, j = 1,\ldots,6$$

The strain–stress connection is then stated in view of engineering constants such as elasticity modulus, E_i (where i = 1, 2, 3); rigidity modulus Gij (where ij = 1, 2, 3); and Poisson's ratio ν_{ij} (where ij = 1, 2, 3).

$$\left[S_{ij}\right] = \begin{bmatrix} \frac{1}{E_1} & -\frac{\nu_{21}}{E_2} & -\frac{\nu_{31}}{E_3} & 0 & 0 & 0 \\ -\frac{\nu_{12}}{E_1} & \frac{1}{E_2} & -\frac{\nu_{32}}{E_3} & 0 & 0 & 0 \\ -\frac{\nu_{13}}{E_1} & -\frac{\nu_{23}}{E_2} & \frac{1}{E_3} & 0 & 0 & 0 \\ 0 & 0 & 0 & \frac{1}{G_{23}} & 0 & 0 \\ 0 & 0 & 0 & 0 & \frac{1}{G_{31}} & 0 \\ 0 & 0 & 0 & 0 & 0 & \frac{1}{G_{12}} \end{bmatrix} \quad (3.1)$$

$$\begin{bmatrix} \varepsilon_1 \\ \varepsilon_2 \\ \varepsilon_3 \\ \gamma_{23} \\ \gamma_{31} \\ \gamma_{12} \end{bmatrix} = \begin{bmatrix} S_{11} & S_{12} & S_{13} & 0 & 0 & 0 \\ S_{12} & S_{22} & S_{23} & 0 & 0 & 0 \\ S_{13} & S_{23} & S_{33} & 0 & 0 & 0 \\ 0 & 0 & 0 & S_{44} & 0 & 0 \\ 0 & 0 & 0 & 0 & S_{55} & 0 \\ 0 & 0 & 0 & 0 & 0 & S_{66} \end{bmatrix} \begin{bmatrix} \sigma_1 \\ \sigma_2 \\ \sigma_3 \\ \tau_{23} \\ \tau_{31} \\ \tau_{12} \end{bmatrix} \quad (3.2)$$

The stress-strain relations are

$$\begin{bmatrix}\sigma_1\\ \sigma_2\\ \sigma_3\\ \tau_{23}\\ \tau_{31}\\ \tau_{12}\end{bmatrix}=\begin{bmatrix}C_{11} & C_{12} & C_{13} & 0 & 0 & 0\\ C_{12} & C_{22} & C_{23} & 0 & 0 & 0\\ C_{13} & C_{23} & C_{33} & 0 & 0 & 0\\ 0 & 0 & 0 & C_{44} & 0 & 0\\ 0 & 0 & 0 & 0 & C_{55} & 0\\ 0 & 0 & 0 & 0 & 0 & C_{66}\end{bmatrix}\begin{bmatrix}\varepsilon_1\\ \varepsilon_2\\ \varepsilon_3\\ \gamma_{23}\\ \gamma_{31}\\ \gamma_{12}\end{bmatrix} \tag{3.3}$$

The nonzero stiffness in Equation (3.3) are

$$C_{11}=\frac{1-\nu_{23}\nu_{32}}{E_2E_3\Delta} \qquad C_{12}=\frac{\nu_{21}+\nu_{31}\nu_{23}}{E_2E_3\Delta}=\frac{\nu_{12}+\nu_{32}\nu_{13}}{E_1E_3\Delta}$$

$$C_{22}=\frac{1-\nu_{13}\nu_{31}}{E_1E_3\Delta} \qquad C_{13}=\frac{\nu_{31}+\nu_{21}\nu_{32}}{E_2E_3\Delta}=\frac{\nu_{13}+\nu_{12}\nu_{23}}{E_1E_2\Delta} \tag{3.4}$$

$$C_{23}=\frac{\nu_{32}+\nu_{12}\nu_{31}}{E_1E_3\Delta}=\frac{\nu_{23}+\nu_{21}\nu_{13}}{E_1E_2\Delta} \qquad C_{33}=\frac{1-\nu_{12}\nu_{21}}{E_1E_2\Delta}$$

$$\text{where } C_{44}=G_{23} \qquad C_{55}=G_{31} \qquad C_{66}=G_{12}$$

$$\Delta=\frac{1-\nu_{12}\nu_{21}-\nu_{23}\nu_{32}-\nu_{31}\nu_{13}-2\nu_{21}\nu_{32}\nu_{13}}{E_1E_2E_3}$$

Formula used to determine equivalent modulus of elasticity is given below:

$$E_x=\frac{F}{\delta}\times\frac{l^3}{48I_z}=tg\beta\times\frac{l^3}{4bh^3} \tag{3.5}$$

Where F = bending force in N; δ = deflection in negative z direction in mm; l = length between two simple supports in mm; β = slope of the (F-δ) curve; b = width of the model in mm; h = thickness of the composite model in mm.

3.2 Three-dimensional finite-element modeling (3-D FEM)

Samples of three different joint types (Type-I, Type-II and Type- III) used in the experimental studies were modeled three dimensionally by using Abaqus CAE 2017. The stress analyses in the adhesively bonded joints using a non-linear finite element method were performed by considering both the geometrical non-linearity and non-linear material behaviors of both adhesives (SBT9244 and DP460) and adherend (AA2024-T3). The dimensions of the samples and boundary conditions used in the finite element analyses were the same as those used in the experimental works.

3.3 Modeling Steps.

The composites' mechanical behavior was investigated using the three-point bending method. The FEA software ABAQUS was employed to model the three-point bending technique.

The following steps are taken in ABAQUS to perform the calculation.

- Creating the part
- Creating and assigning material
- Instancing the part
- Creating steps
- Applying Loading and Boundary Condition
- Meshing the part

3.4 Creating the Part:

A 3D deformable part For Adhered (Type I, Type II, and Type III) of 100mm length, 5.25mm thickness and 25mm Width. For Adhesive (Type I, Type II) of 25mm length, 0.15mm thickness and 25mm width. For Type III Adhesive 15mm length, 0.15mm thickness, 25mm width and another one is 5mm length, 0.15mm thickness, 25mm width [10].

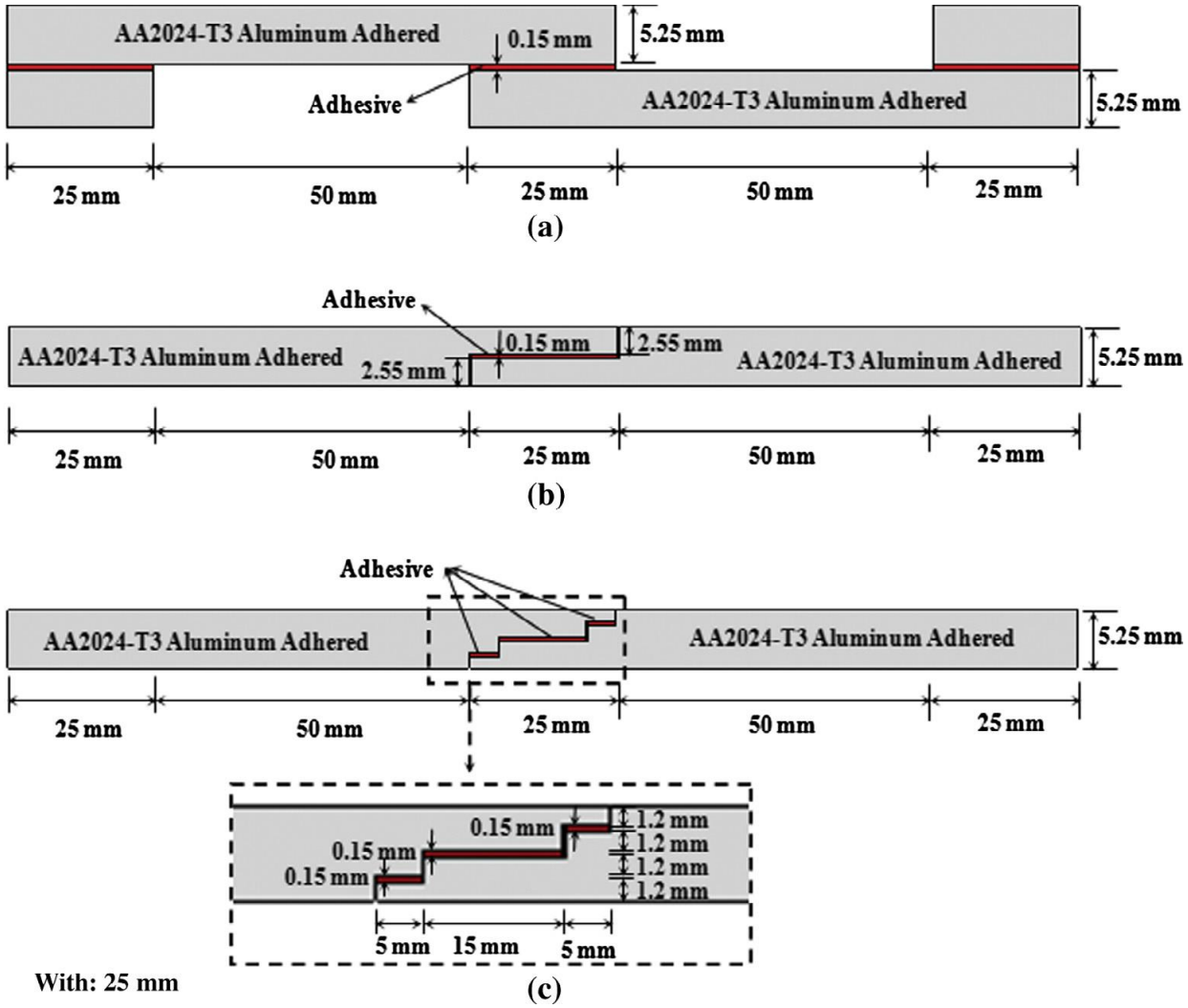

Figure 3.1: Geometric parameters of adhesively bonded joints; (a) single lap joint (Type-I), (b) one step lap joint (Type-II), (c) three step lap joint (Type-III).

3.5 Creating and assigning material:

In this study, DP460, a two-part paste stiff adhesive produced by 3 M, and SBT 9244, a film type flexible adhesive, were used as adhesives. AA2024-T3 aluminum alloy, a well-known material used in the aerospace and automotive industry due to its low density [10].

Table 1. Material properties of the adherend and adhesives

Material	AA2024-T3	SBT9244	DP460
E (MPa)	72400 ± 530	82 ± 4	2077 ± 47
v	0.33	0.35	0.38
σ_t (MPa)	482 ± 12	20.9 ± 0.7	44.6 ± 1.2
ε_t (mm/mm)	0.1587	0.945	0.0428

Table 2. Experimental parameters for adhesively-bonded joints.

Specimen	Joint type	Adhesive area (mm^2)
SBT9244-adhesively bonded single lap joint	Type I a	625
DP460-adhesively bonded single lap joint	Type I b	625
SBT9244-adhesively bonded one-step lap joint	Type II a	625
DP460-adhesively bonded one-step lap joint	Type II b	625
SBT9244-adhesively bonded three-step lap joint	Type III a	625
DP460-adhesively bonded three-step lap joint	Type III b	625

3.6 Creating the Model:

3.6.1 Model-1 (Type Ia):

In Adhered we use two adhered upper and lower adhered AA2024-T3. The length of adhered 100 mm, thickness 5.25 mm and width 25 mm and we use adhesive SBT9244, the length of adhesive 25 mm, thickness 0.15 mm and width 25mm.

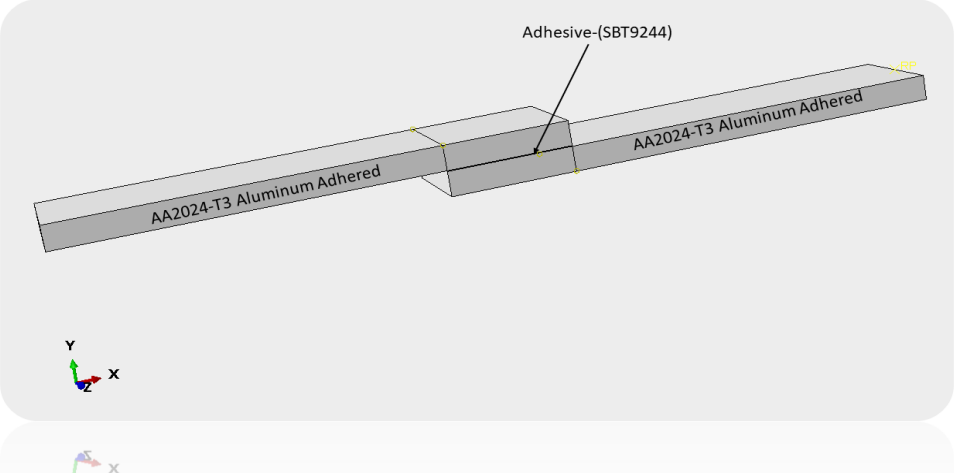

Figure 3.2: SLJ with SBT9244 adhesive.

3.6.2 Model-2 (Type Ib):

In Adhered we use two adhered upper and lower adhered AA2024-T3. The length of adhered 100 mm, thickness 5.25 mm and width 25 mm and we use stiff adhesive DP460, the length of adhesive 25 mm, thickness 0.15 mm and width 25mm.

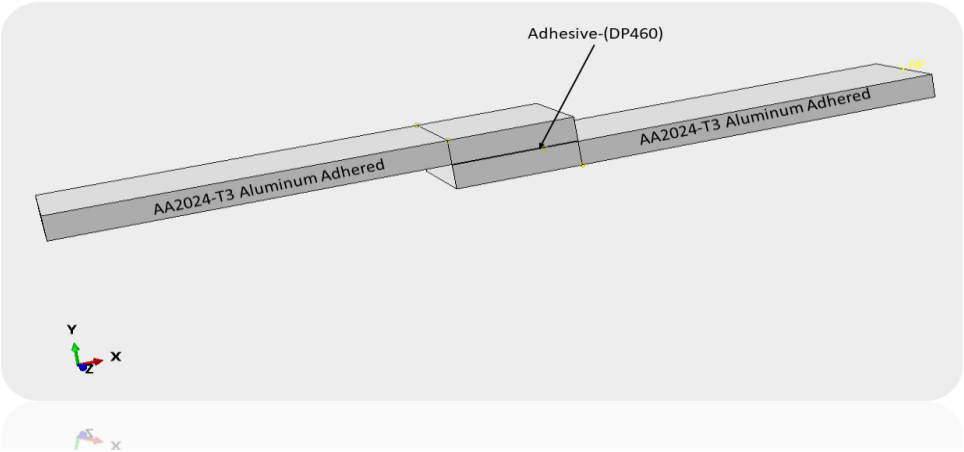

Figure 3.3: SLJ with DP460 adhesive.

3.6.3 Model-3 (Type IIa):

In Adhered we use two one step adhered upper and lower adhered AA2024-T3. The length of adhered 100 mm, thickness 5.25 mm and width 25 mm and we use adhesive SBT9244, the length of adhesive 25 mm, thickness 0.15 mm and width 25mm.

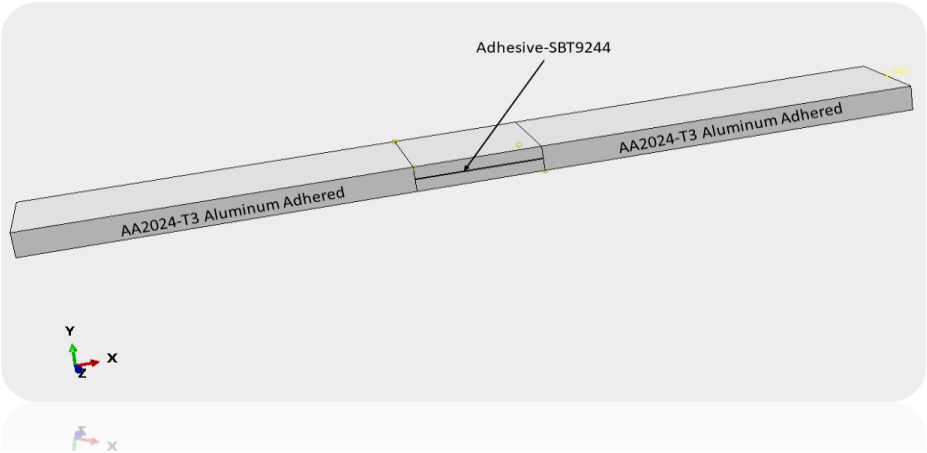

Figure 3.4: OSLJ with SBT9244 adhesive.

3.6.4 Model-4 (Type IIb):

In Adhered we use two one step adhered upper and lower adhered AA2024-T3. The length of adhered 100 mm, thickness 5.25 mm and width 25 mm and we use stiff adhesive DP460, the length of adhesive 25 mm, thickness 0.15 mm and width 25mm.

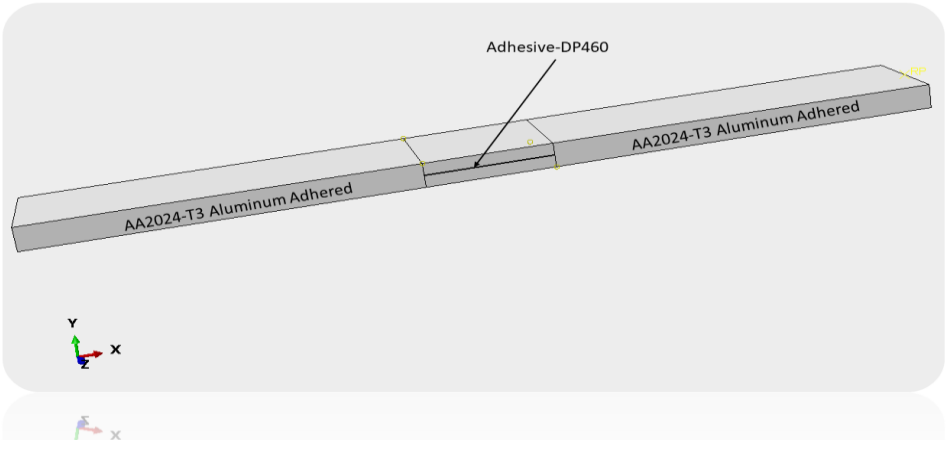

Figure 3.5: OSLJ with DP460 adhesive.

3.6.5 Model-5 (Type IIIa):

In Adhered we use two three steps adhered upper and lower adhered AA2024-T3. The length of adhered 100 mm, thickness 5.25 mm and width 25 mm and we use adhesive SBT9244, the length of adhesive 15 mm, thickness 0.15 mm and width 25mm another adhesive is 5mm, 0.15mm and 25mm.

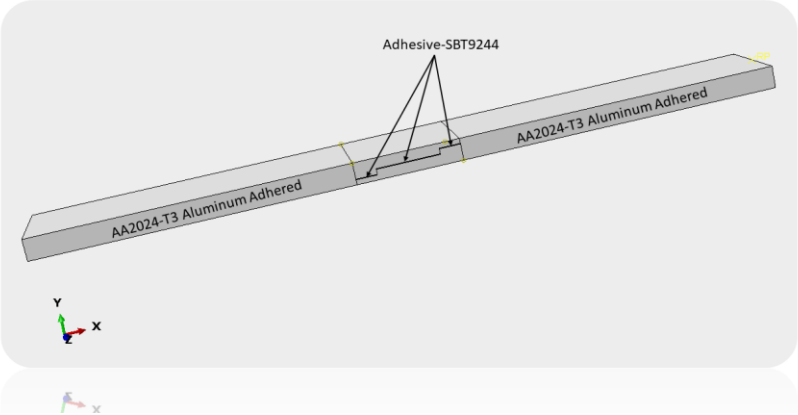

Figure 3.6: TSLJ with SBT9244 adhesive.

3.6.6 Model-6 (Type IIIb):

In Adhered we use two three steps adhered upper and lower adhered AA2024-T3. The length of adhered 100 mm, thickness 5.25 mm and width 25 mm and we use stiff adhesive DP460, the length of adhesive 15 mm, thickness 0.15 mm and width 25mm another adhesive is 5mm, 0.15mm and 25mm.

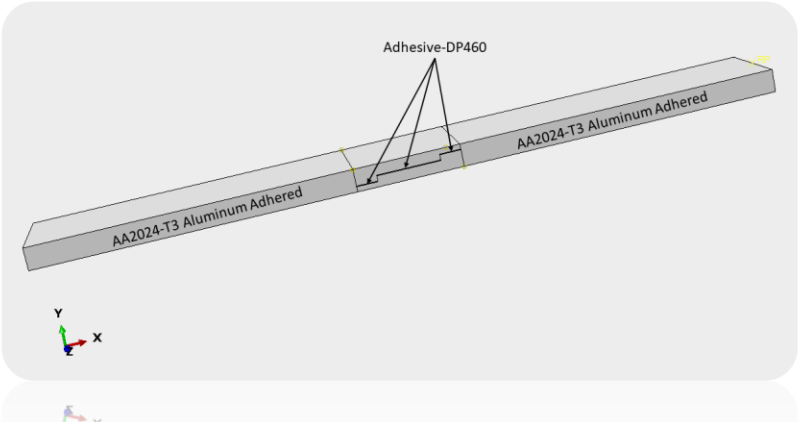

Figure 3.7: TSLJ with DP460 adhesive.

3.7 Instancing the part:

The part was instanced to be a dependent (mesh) on part instance before setting any boundary conditions or meshes.

3.8 Creating steps:

There have been two steps created. The first is the initial step, and the second is the loading step. In the initial step, the boundary condition was applied, and in the loading step, the load was applied. Time period for the loading step is 11.

3.9 Applying Loading and Boundary Condition:

At first we create three sets (Left Face, Right Face and Reference Plane (RP)) and one surface (Right Surface).Boundary condition applied at Left face and Load applied at Reference plane.
We find that maximum failure load in this section.

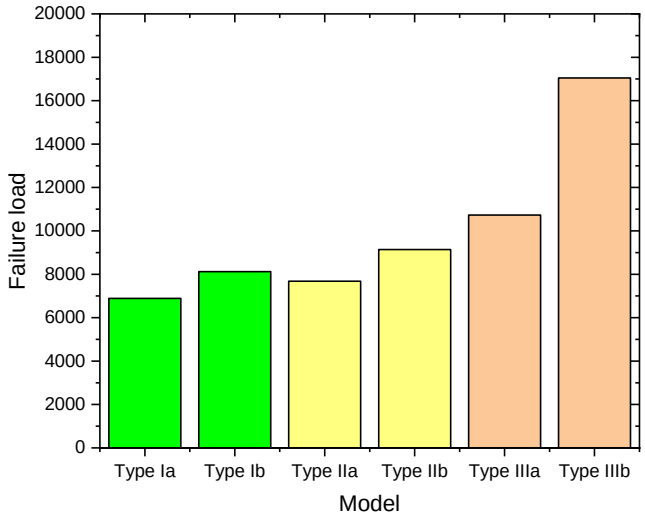

Figure 3.8: Maximum failure load.

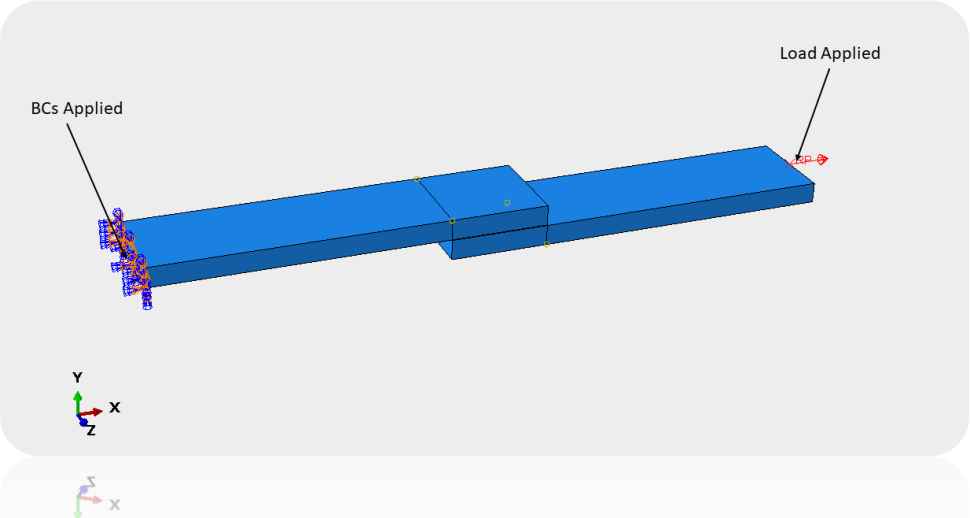

Figure 3.9: Load and boundary condition.

3.10 Meshing the part:

In this part we using part by part regions mesh and many elements size respectively, then the total part is meshed. We use number of element 5 double bias of adhesive and adhered 0.2 double bias and 0.5 none bias and total part element size 1 none bias. Finally, the job is submitted for the analysis.

Element type of the meshing is C3D8R linear hexahedral i.e, the element is an 8-node linear brick, reduced integration with an hourglass control element.

- Total number of elements Type Ia is 63750.
- Total number of elements Type Ib is 56250.
- Total number of elements Type IIa is 69875.
- Total number of elements Type IIb is 55275.
- Total number of elements Type IIIa is 54175.
- Total number of elements Type IIIb is 32550.

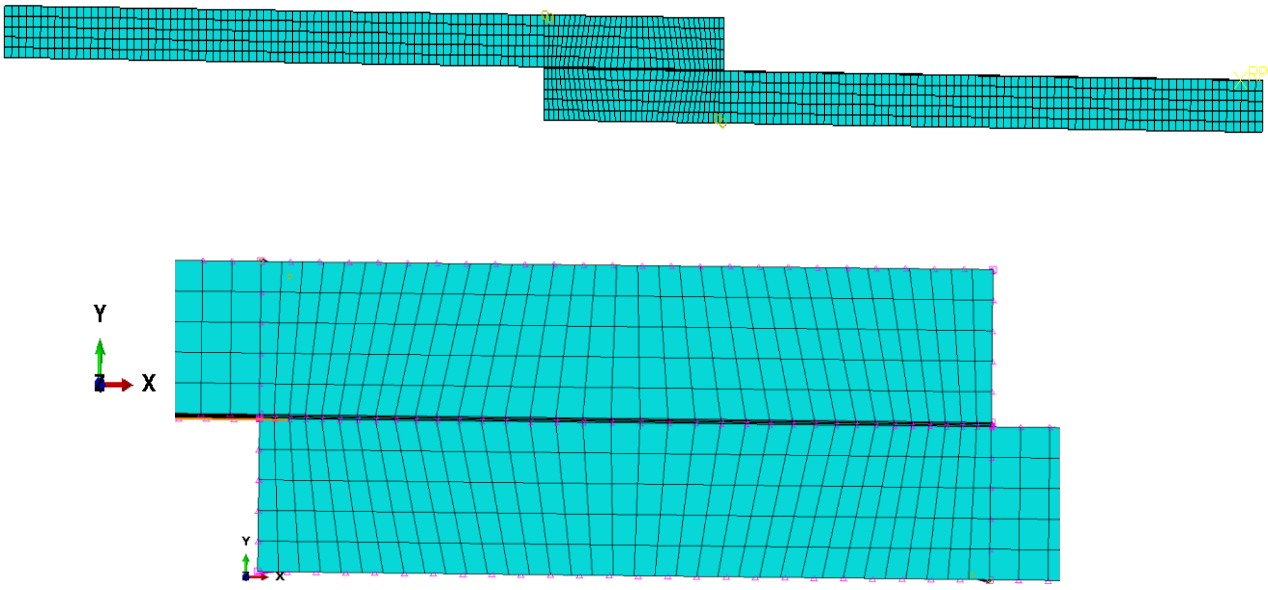

Figure 3.10: Finite element analyses assemble models of adhesively bonded joint SLJ.

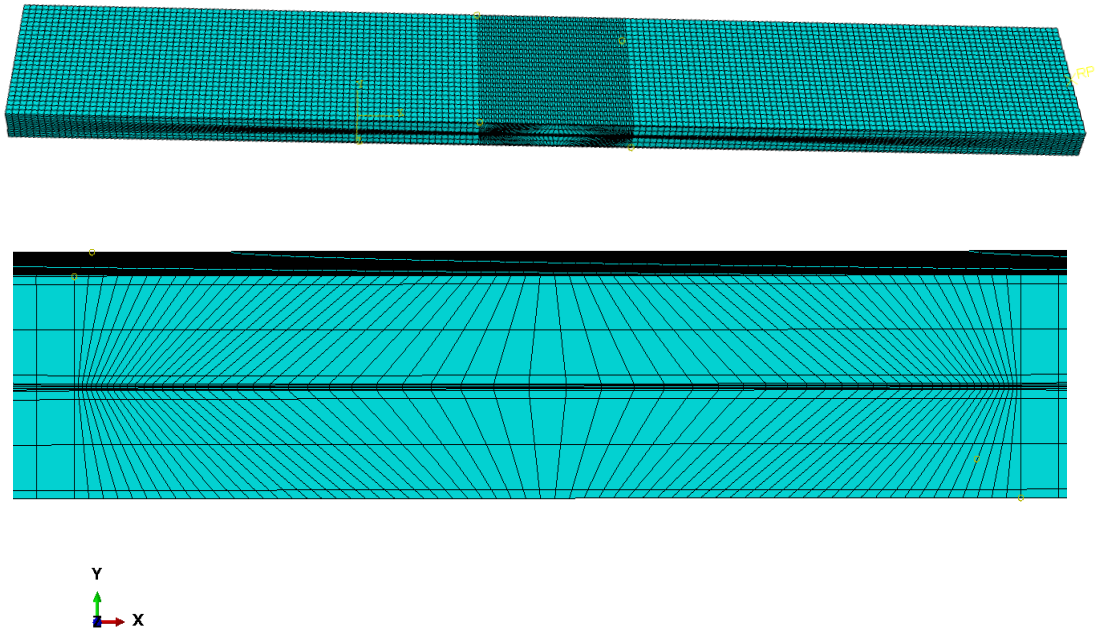

Figure 3.11: Finite element analyses assemble models of adhesively bonded joint OSLJ.

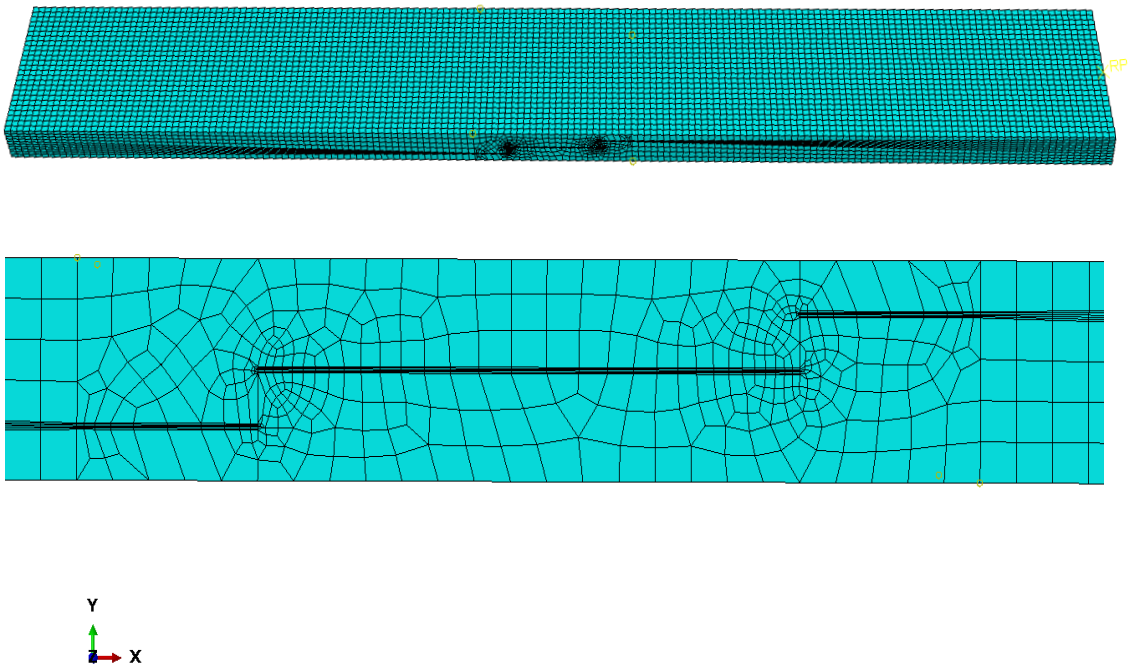

Figure 3.12: Finite element analyses assemble models of adhesively bonded joint TSLJ.

CHAPTER 4 RESULT & DISCUSSION

4.1 Mesh Sensitivity Analysis

Single-lap joints are by far the most widely used adhesive joints and have been the subject of considerable research over the years so we are show SLJ mesh dependency. [25]

Mesh dependency test of the analysis was performed using elements of six different sizes varying from the impact area. The number of elements were 1120, 2980, 16866, 66861, 77265 and 56250. For the dependency of the mesh the von-mises stress vs overlap length curve was compared for different meshes. From the stress comparison curves in Fig. 4.1, for the all number of elements are approximately same. The maximum deviation of the no of element 77265 are also negligible. So, it is safe to assume that for these element sizes the analysis is mesh independent and analysis can be performed using any one of these element sizes. So, for the analysis using the region native mesh (the number of elements is 56250) was taken as average and minimum stress also to get suitable results. Maximum value of stress of SBT9244 Type Ia is 10.5 MPa and DP460 Type Ib is 36.5MPa.

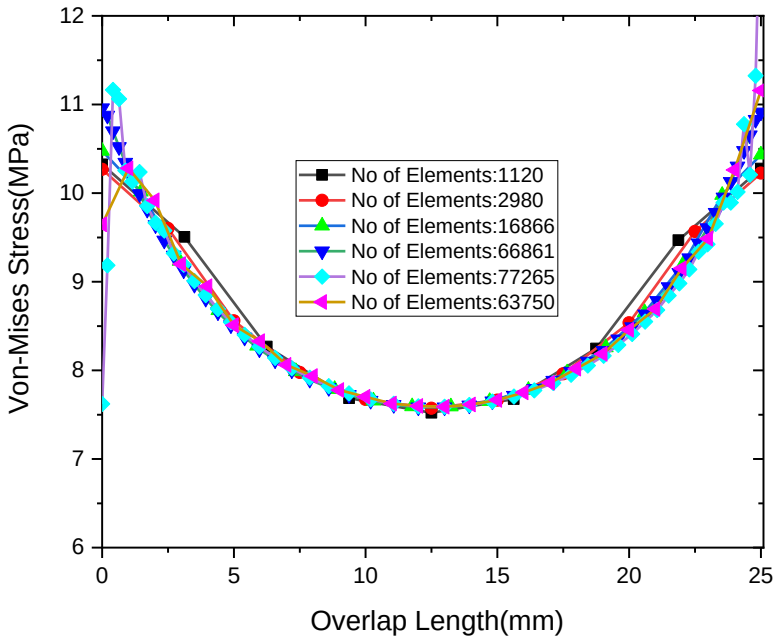

Figure 4.1: Mesh sensibility analysis

4.2 Model Validation

Single-lap joints are by far the most widely used adhesive joints and have been the subject of considerable research over the years so we are show SLJ Model compare only [28].

The modelling used in this work was performed by Salih Akpinar [10]. A numerical simulation of adhesive bonded joints composite material was carried out. Data from the previously mentioned research study was extracted using the origin software. Then the result of the simulation was compared with the result extracted from the research paper. Peel stress along Y-axis and overlap length along X-axis is considered as the parameter of comparison. Figure 4.2 illustrates the comparison. The comparison shows that the error is quite minimal some deviation occurs starting and ending point, indicating that the simulation method is accurate.

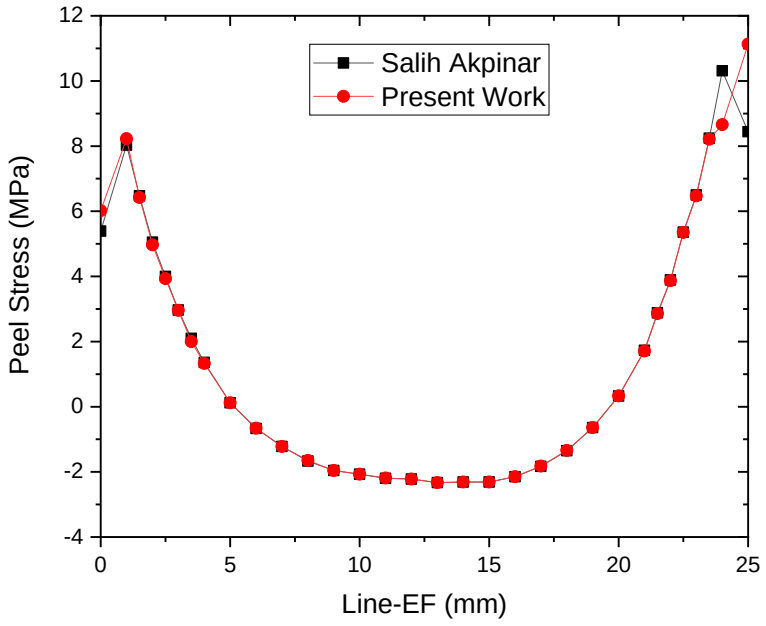

Figure 4.2: Compare between present study and previous research

Table 3. Model Validation

	Stress (MPa)		
Displacement Line-EF (mm)	Salih Akpinar	Present Work	Error (%)
0	5.39	6.02	11.69
1	8.03	8.23	2.49
1.5	6.47	6.42	0.77
2	5.05	4.97	1.58
2.5	4	3.93	1.75
3	2.97	2.96	0.33
3.5	2.1	2	4.76
4	1.36	1.33	2.21
5	0.12	0.12	0.06
6	-0.67	-0.66	1.49
7	-1.22	-1.22	0.05
8	-1.67	-1.65	1.2
9	-1.96	-1.96	0.03
10	-2.07	-2.07	0.03
11	-2.2	-2.19	0.46
12	-2.22	-2.22	0.07
13	-2.33	-2.33	0.08
14	-2.31	-2.31	0.09
15	-2.31	-2.31	0.06
16	-2.15	-2.15	0.05
17	-1.83	-1.823	0.39
18	-1.35	-1.343	0.52
19	-0.64	-0.64	0.05
20	0.33	0.332	0.61
21	1.73	1.71	1.15
21.5	2.88	2.86	0.69
22	3.89	3.87	0.51
22.5	5.36	5.35	0.18
23	6.5	6.47	0.46
23.5	8.24	8.21	0.36
24	10.31	8.66	16
25	8.44	11.132	31.89

4.3 Maximum Failure Load:

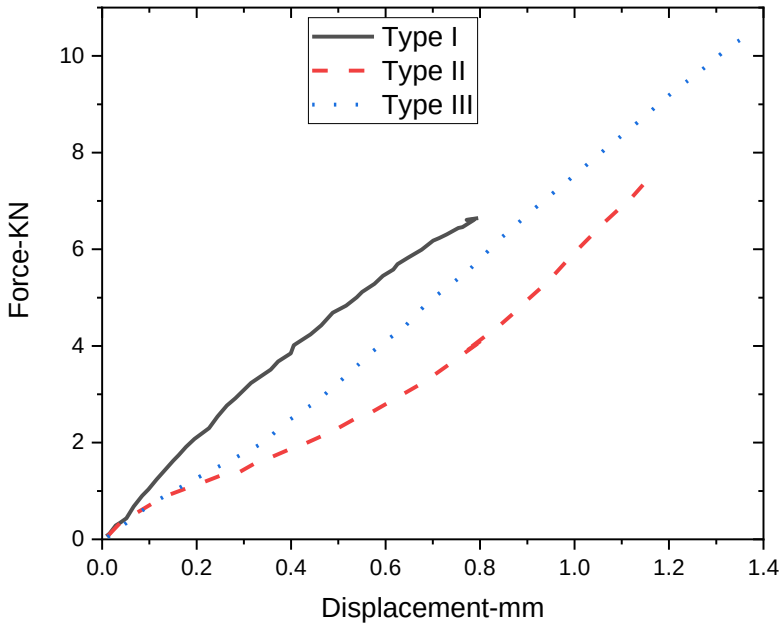

Figure 4.3: Maximum failure load of SBT9244 adhesive.

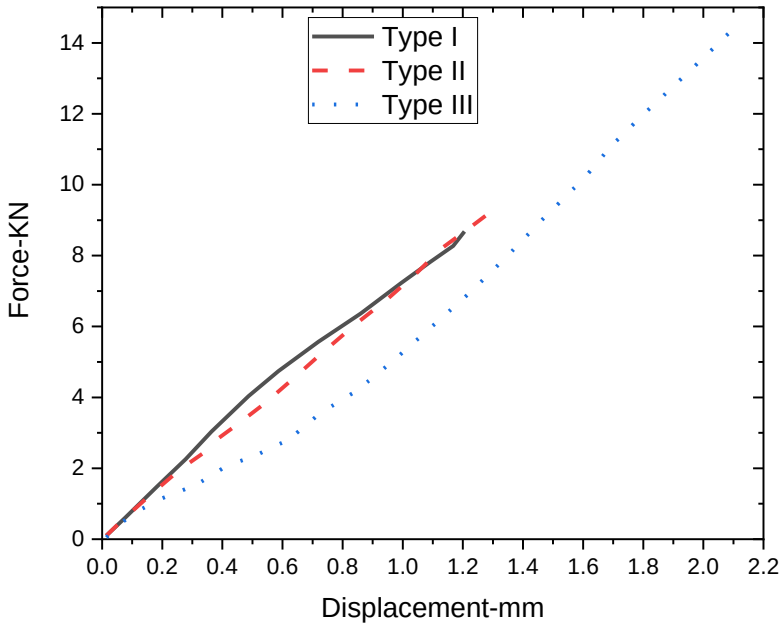

Figure 4.4:Maximum failure load of DP460 adhesive.

4.4 Discussion About Present Work:

Finite Element Analysis software ABAQUS 2017 has been used to investigate stress, load-displacement response in Adhesive joints of the composite structures. All parameters are plotted by changing the layup arrangements of the composites. Equivalent modulus of elasticity of the composite structures has been calculated by using equation available in the literature. In this case, FEM is used to get approximate solutions to various equations in physical situations with boundary conditions. Each element computes approximate solutions, which are then merged to produce the outcome. The contours and graphical representations are illustrated and discussed below.

4.5 Stress Analysis:

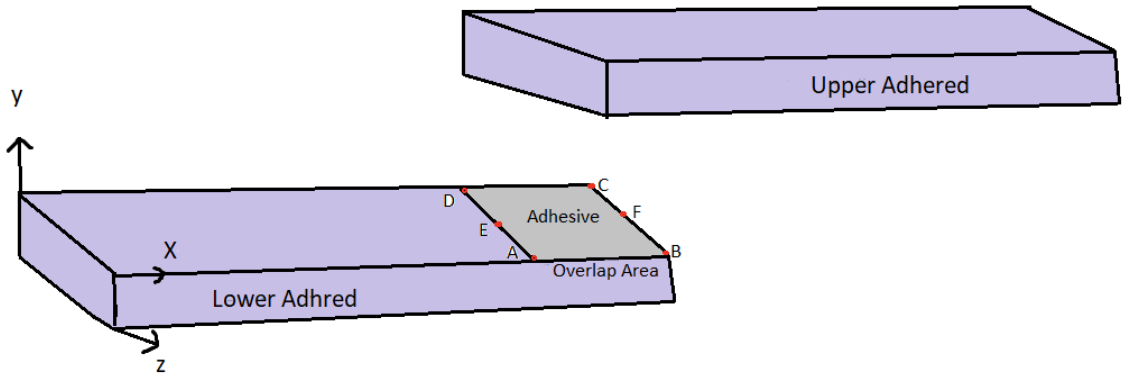

Figure 4.5: Critical failure surfaces of the joint samples bonded with adhesive.

4.5.1 Type-Ia:

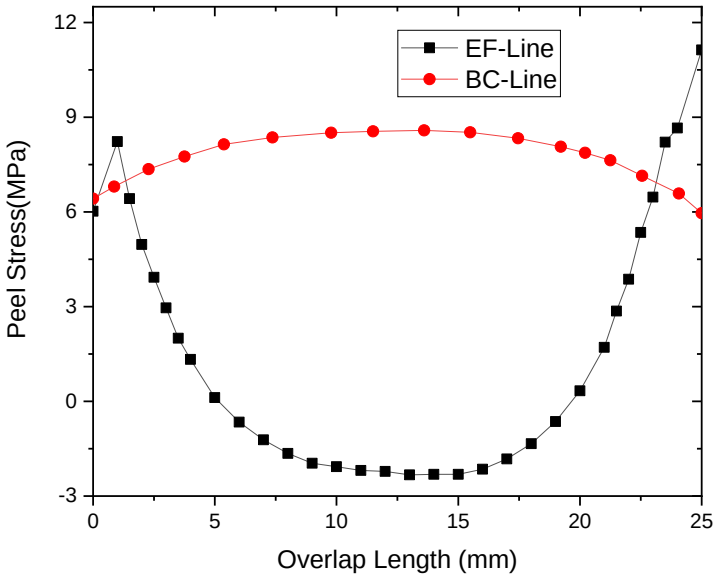

Figure 4.6: Comparison of the stress distributions in the adhesive layer along EF line and BC Line for SLJ joint bonded with SBT9244 adhesive peel stress (σ_y)

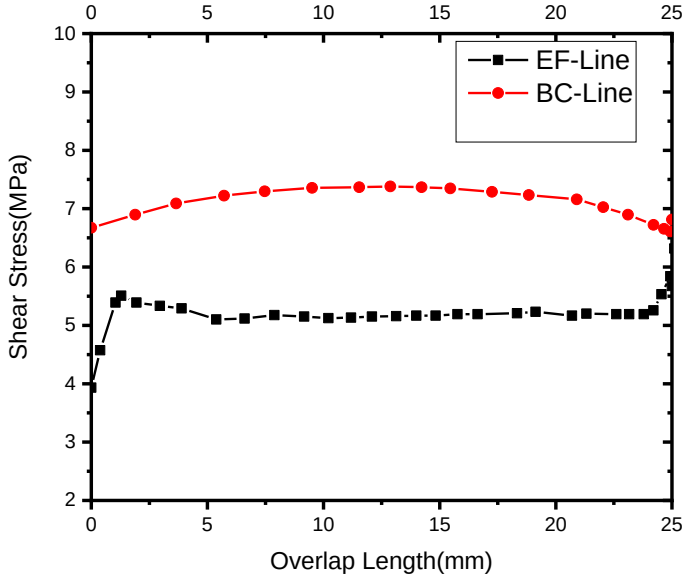

Figure 4.7: Comparison of the stress distributions in the adhesive layer along EF line and BC Line for SLJ joint bonded with SBT9244 adhesive peel stress (σ_y)

4.5.2 Type-Ib:

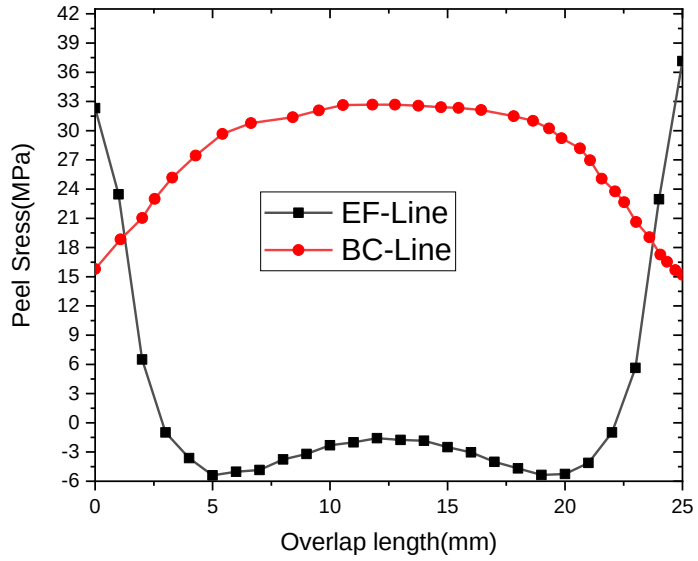

Figure 4.8: Comparison of the stress distributions in the adhesive layer along EF line and BC Line for SLJ joint bonded with SBT9244 adhesive peel stress (σ

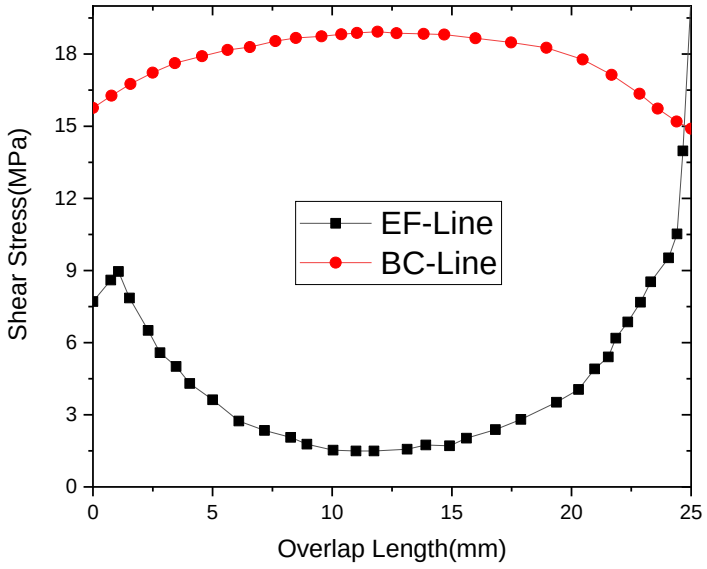

Figure 4.9: Comparison of the stress distributions in the adhesive layer along EF line and BC Line for SLJ joint bonded with SBT9244 adhesive peel stress (σ_y)

4.5.3 Type-IIa:

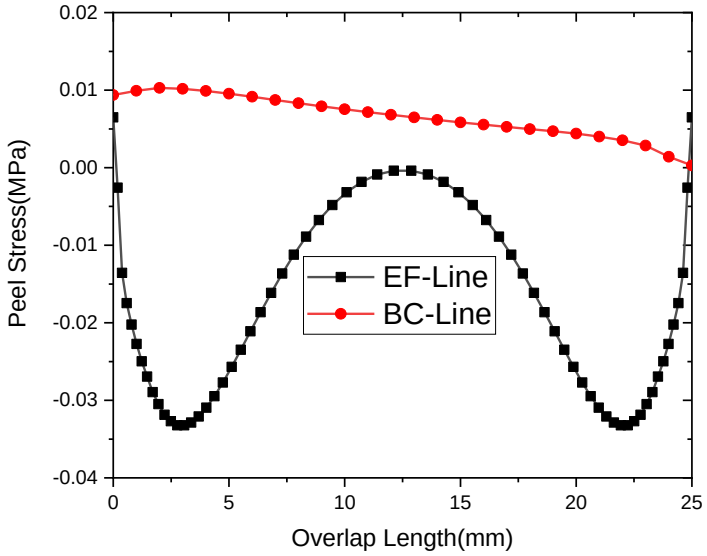

Figure 4.10: Comparison of the stress distributions in the adhesive layer along EF line and BC Line for SLJ joint bonded with SBT9244 adhesive peel stress (σ_y)

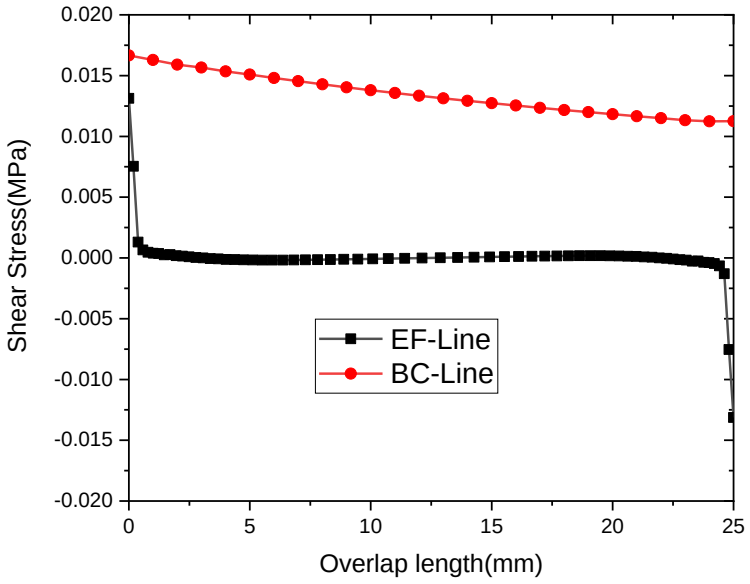

Figure 4.11: Comparison of the stress distributions in the adhesive layer along EF line and BC Line for SLJ joint bonded with SBT9244 adhesive peel stress (σ_y)

4.5.4 Type-IIb:

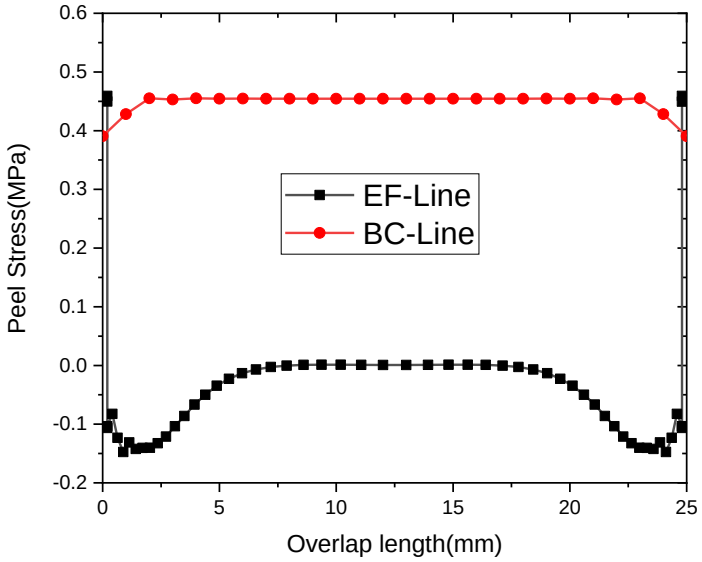

Figure 4.12: Comparison of the stress distributions in the adhesive layer along EF line and BC Line for SLJ joint bonded with SBT9244 adhesive peel stress (σ_y)

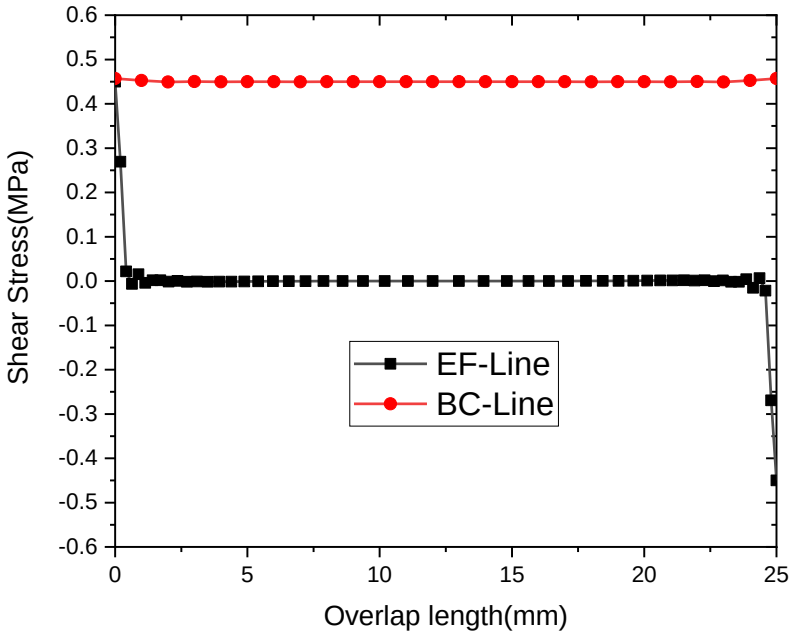

Figure 4.13: Comparison of the stress distributions in the adhesive layer along EF line and BC Line for SLJ joint bonded with SBT9244 adhesive peel stress (σ_y)

4.5.5 Type-IIIa:

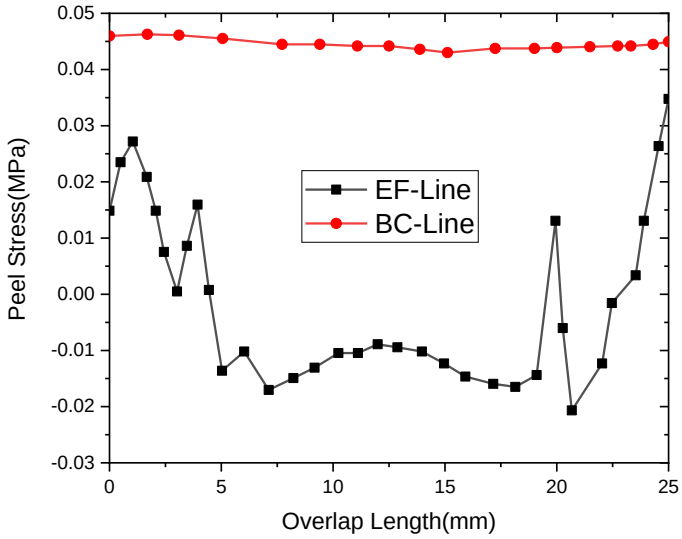

Figure 4.14: Comparison of the stress distributions in the adhesive layer along EF line and BC Line for SLJ joint bonded with SBT9244 adhesive peel stress (σ_y)

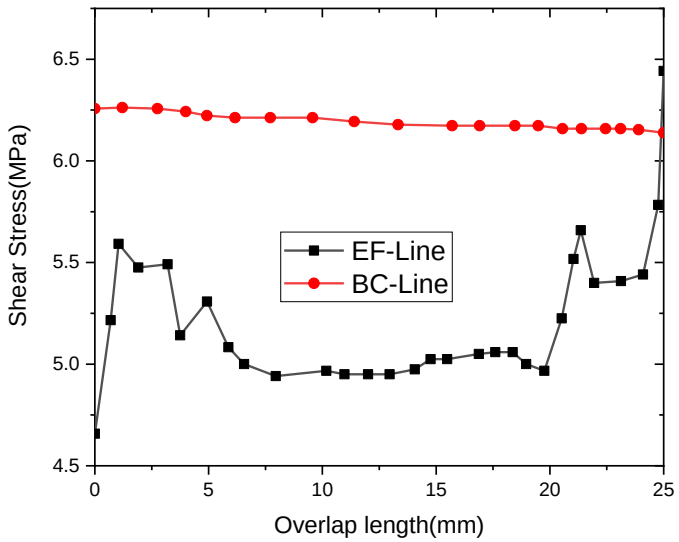

Figure 4.15: Comparison of the stress distributions in the adhesive layer along EF line and BC Line for SLJ joint bonded with SBT9244 adhesive peel stress (σ_y)

4.5.6 Type-IIIb:

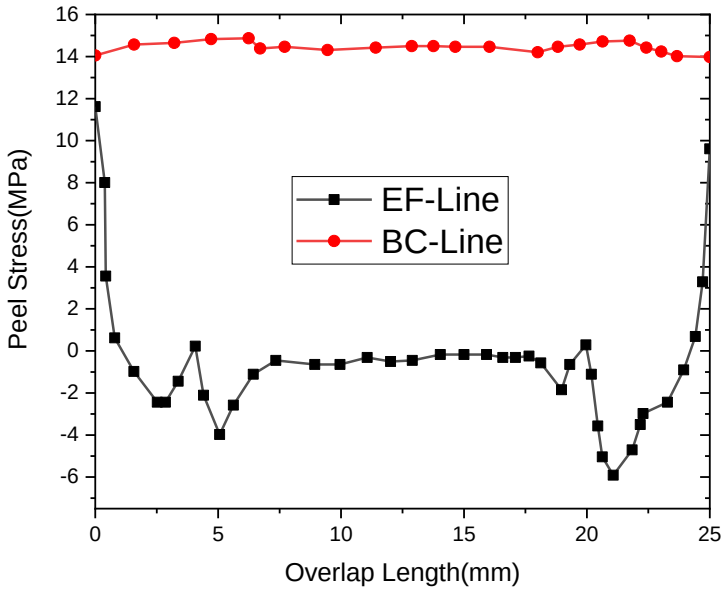

Figure 4.16: Comparison of the stress distributions in the adhesive layer along EF line and BC Line for SLJ joint bonded with SBT9244 adhesive peel stress (σ_y)

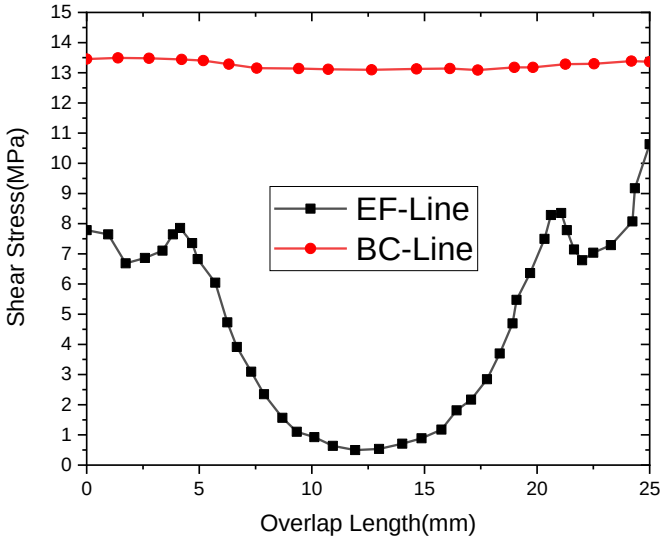

Figure 4.17: Comparison of the stress distributions in the adhesive layer along EF line and BC Line for SLJ joint bonded with SBT9244 adhesive peel stress (σ_y)

Single-lap joints are by far the most widely used adhesive joints and have been the subject of considerable research over the years. In single-lap bonded joints the stresses are maximum at the edges, where failure usually begins, while in the center stresses are the minimum. Three samples of Type-Ia, Type-IIa, Type-IIIa, Type-Ib, Type-IIb and Type-IIIb were subjected to tensile loading until failure. Type-Ia peel stress the comparison shows that the error is quite minimal some deviation occurs starting and ending point.

Following to the finite element analysis (FEA) values of Type-I, Type-II and Type-III joints given in (Figure 3.8: Maximum failure load.). The results of the numerical analysis study show that critical loci for failure are the interface between adhesive layer and upper adherend (the surface ABCD), see (Figure 4.5: Critical failure surfaces of the joint samples bonded with adhesive.). Finite element analyses (FEA) were accomplished for the joint types obtained by using flexible SBT9244 adhesive having the same bonding area (Type-Ia, Type-IIa, Type-IIIa) under a tensile load of 3000 N, while, they were conducted out for the joint types obtained by using stiff DP460 adhesive (Type-I b, Type-II b, Type-III b) under a load of 4000 N (in these types of specimen joints experiments this is the half load of minimum failure load). A comparison of peel and shear which are more effective than other stresses on failure, stress distributions occurring on the adhesive layer along the midline of the adhesive layer (at EF line).
If these graphs are examined, stress concentrations exist at the edges of the overlap area with a maximum value at point F. The peel stress ordination of the joints bonded by SBT9244 given in those stress comparison Fig. exhibits that for Type-I a joint, peel stresses show tensile character at the edges of the overlap area, while, they reducing towards the center and gain compressive character at the portion close to the center. Since the effect of moment formed due to the irrelevant loading in Type-I a joint decreased in Type-II a, stresses formed at the portions close to the center are nearly zero for this joint type.

Moreover, machining of steps at the portions close to the edges of the overlap area for Type-III a joint decreased the peel stresses, formed at the edges of the overlap area, which are very effective in initiating the damage and shifted these stresses towards the center of the overlap area, see (Figure 4.14: Comparison of the stress distributions in the adhesive layer along EF line and BC Line for SLJ joint bonded with SBT9244 adhesive peel stress (σ_y). In the meanwhile, along the overlap length (EF line),

shear stresses are maximum at point F, while it is minimum at point E. The difference in the stress values formed at the both edges of the overlap area in Type-I a and Type-II a joint is high. However, it was observed that the difference in stress values of the edges of the Type III-a joint decreased and this type of joint demonstrates more homogenous stress distribution.
As seen from stiff adhesive the peel stress distributions of the three joint types bonded by DP460 adhesive shows that stress concentrations formed at the edges of the overlap area and stress values reached the maximum value at point F. While, the peel stresses showed compressive character for Type-I b joint at the middle part of the overlap area, they are close to zero for Type-II b and Type-III b joints. Meanwhile, shear stress does not show a uniform distribution along the overlap length, EF line. For all types, shear stress distributions are the maximum at point F, while they are the minimum in the middle of the overlap area.

Finally, shear stresses formed in the Type III b moved from edges of the overlap area to the inner areas. For Type-I a joint, it is seen that peel stresses had tensile character at the edges of the overlap area, whereas they showed compression character towards the center and took values close to zero at the portions near to the center. As seen peel stress and shear stress distributions on the adhesive layer along BC line show that for Type-I joint, stress values are not uniform along this line, i.e., maximum at the center (point F) and minimum at the edges (points B and C) as well as the values showed great difference between center and the edges.

Though, such difference between center and the edges along the width decreased significantly for Type-II joint and there is nearly no difference in stress values for Type-III joint, as seen from the homogeneous distribution. Another point that should be considered is that, at point F, the value of peel stress (an effective parameter for the initiation of the damage on adhesive layer) decreased in Type II and Type-III compared to Type I. On the other hand, in Type II and Type III joints, not only peel stresses but also shear stresses reduced. However, the amount of decrease in stress values observed for Type II and Type-III joints was not the same, while the highest decrease occurred in Type-III. If it is considered that the reduction in the stress values raised the load carrying capacity of the joint, it can be realized that the results obtained from finite element analyses are coherent with those obtained from experimental work.

4.6 Contour Map:

4.6.1 Type-Ia:

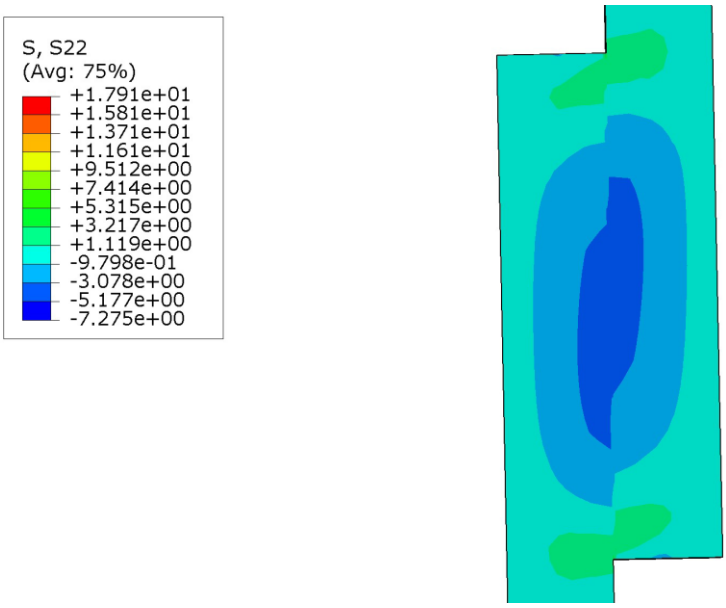

Figure 4.18: Y direction peel stress contour map under unit tensile loading of adhesive SBT9244

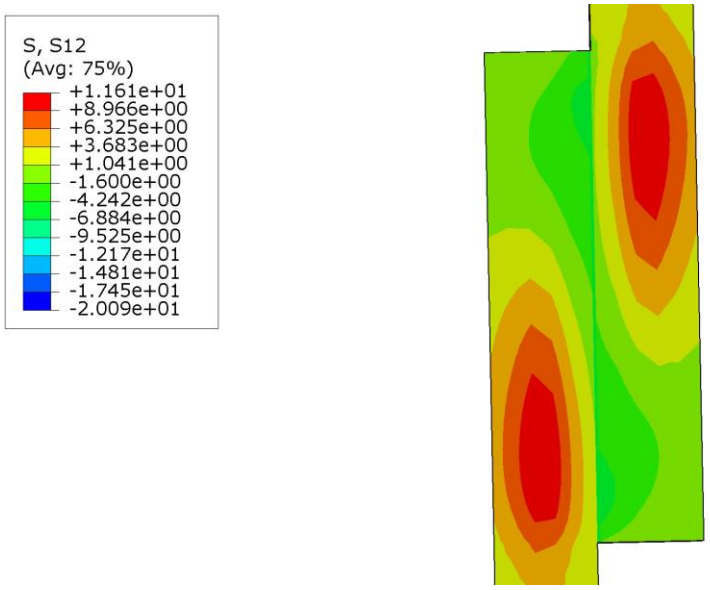

Figure 4.19: XY direction Shear stress contour map under unit tensile loading of adhesive SBT9244

4.6.2 Type-Ib:

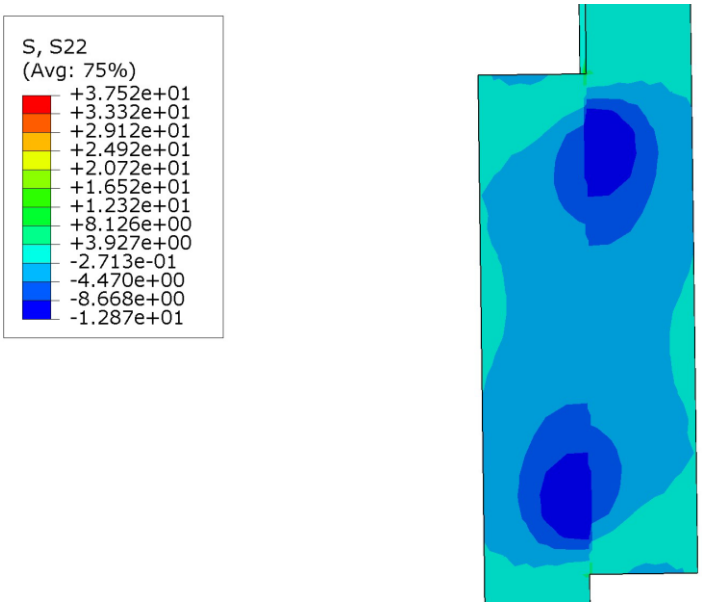

Figure 4.20: Y direction peel stress contour map under unit tensile loading of adhesive DP460

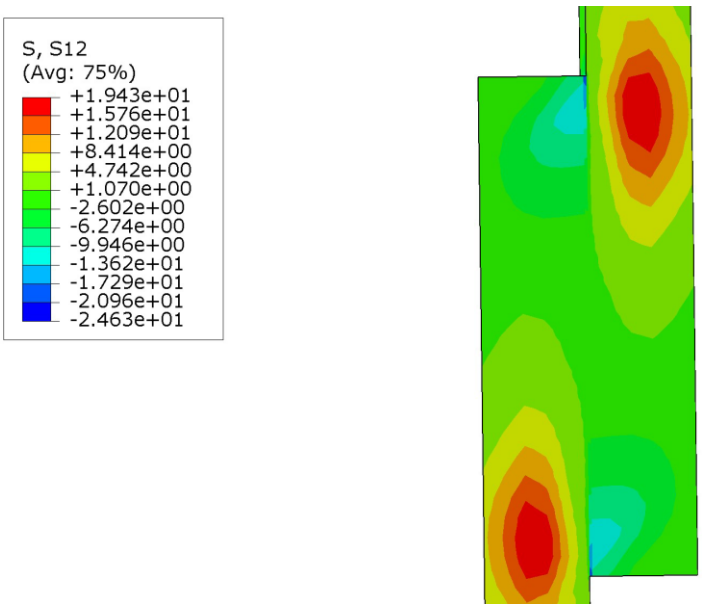

Figure 4.21: XY direction shear stress contour map under unit tensile loading of adhesive DP460

4.6.3 Type-IIa:

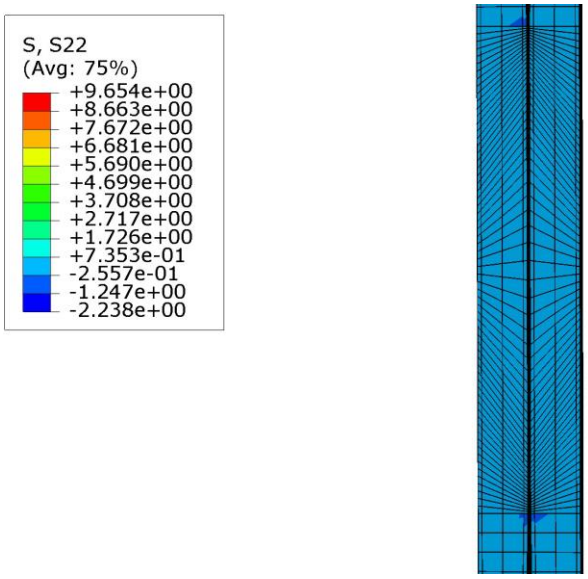

Figure 4.22: Y direction peel stress contour map under unit tensile loading of adhesive SBT9244

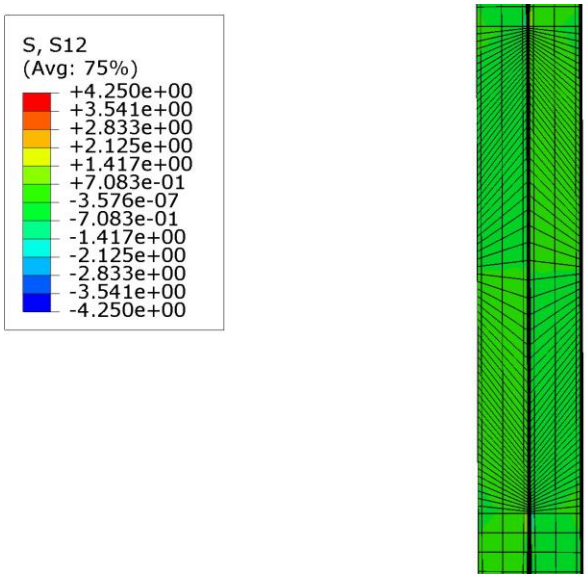

Figure 4.23: XY direction shear stress contour map under unit tensile loading of adhesive SBT9244

4.6.4 Type-IIb:

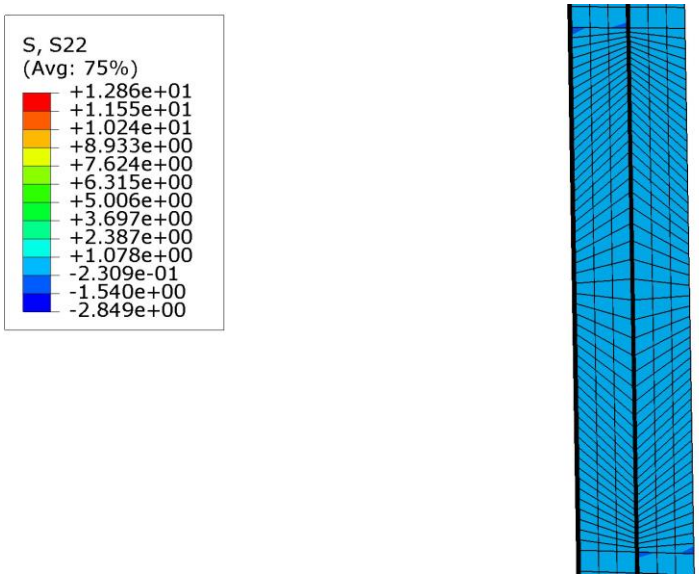

Figure 4.24: Y direction peel stress contour map under unit tensile loading of adhesive DP460

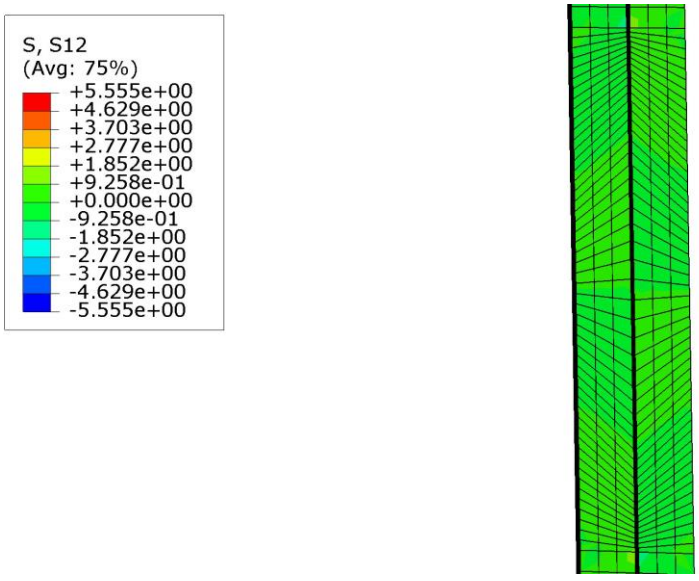

Figure 4.25: XY direction shear stress contour map under unit tensile loading of adhesive DP460

4.6.5 Type-IIIa:

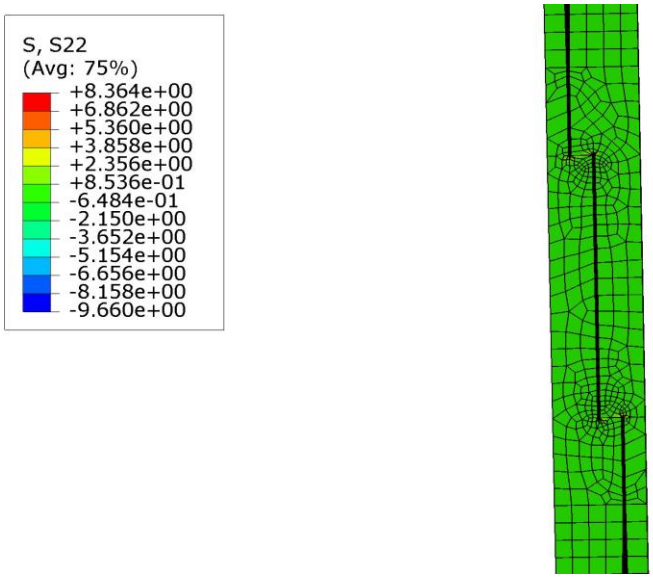

Figure 4.26: Y direction peel stress contour map under unit tensile loading of adhesive SBT9244

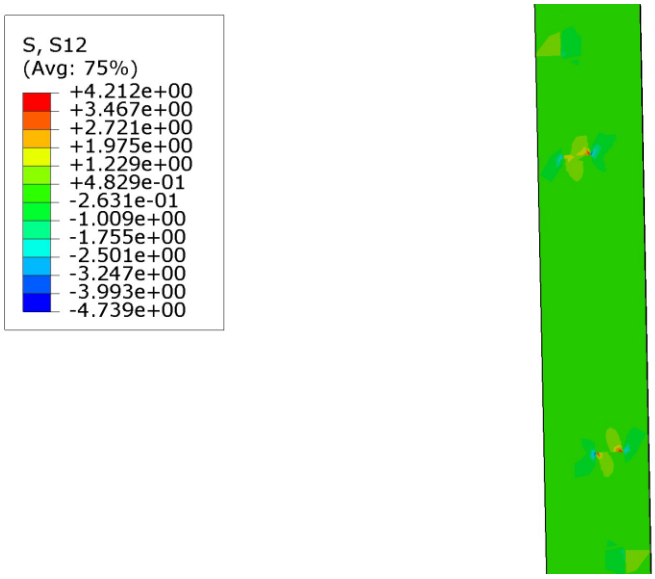

Figure 4.27: XY direction shear stress contour map under unit tensile loading of adhesive SBT9244

4.6.6 Type-IIIb:

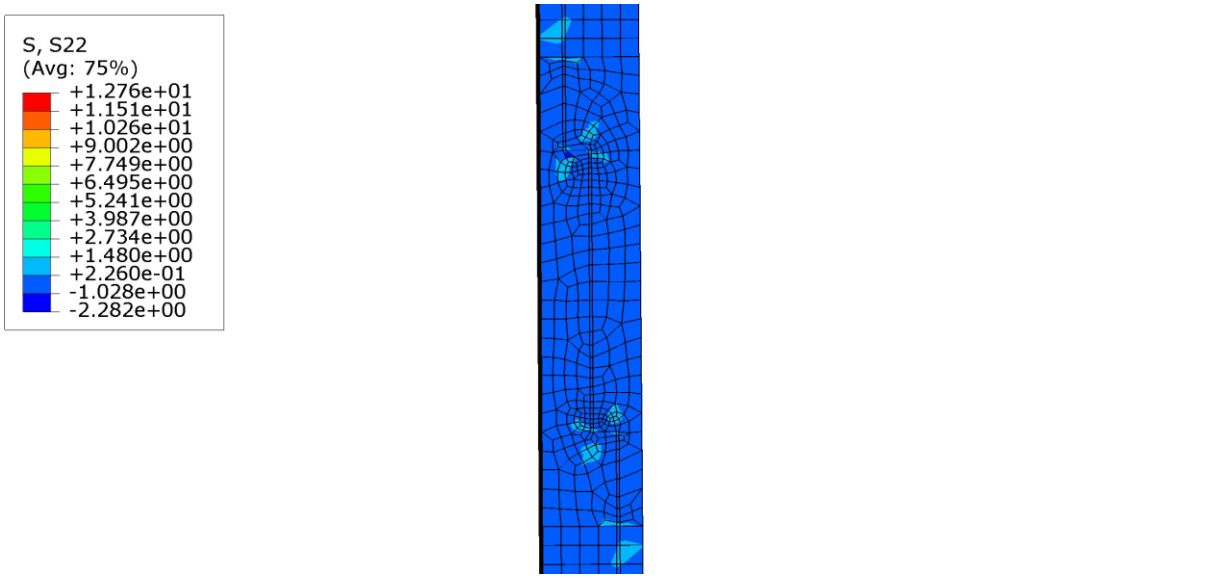

Figure 4.28: Y direction peel stress contour map under unit tensile loading of adhesive DP460

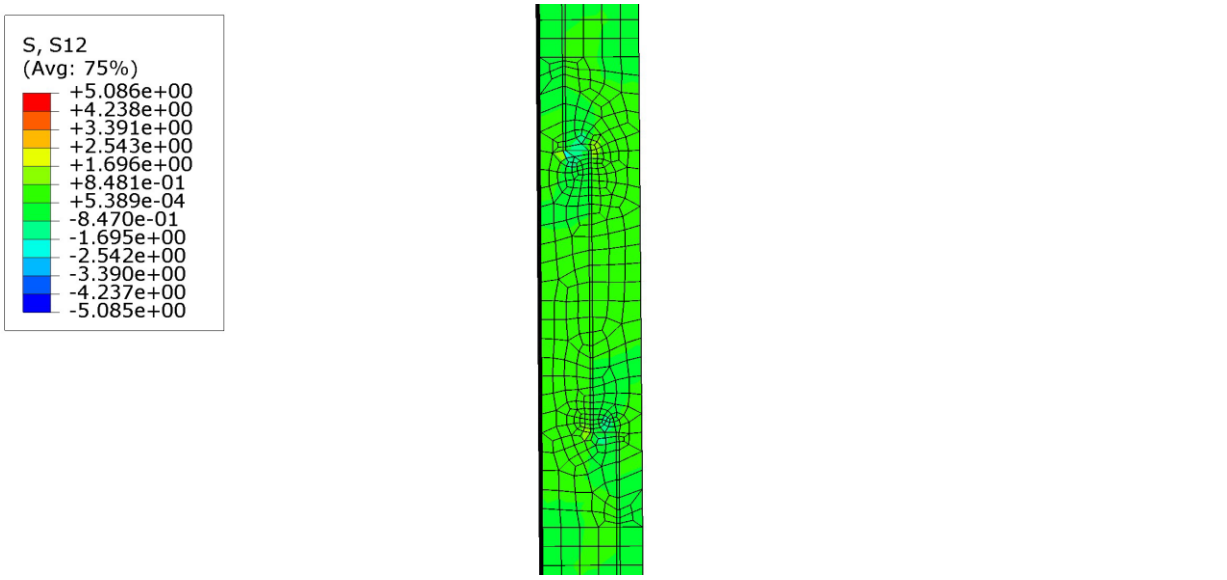

Figure 4.29: XY direction shear stress contour map under unit tensile loading of adhesive DP460

CHAPTER 5 CONCLUSION

5.1 Conclusion:

In this Numerical Study, the mechanical behaviors of three different joint types (SLJ, OSLJ and TSLJ) subjected to tensile loading were investigated numerically. Accordingly, the following conclusions can be drawn:

- Using a linear material model and nonlinear geometry, along with approximate but near accurate measurements and boundary condition mimicry and a verified mesh density, one can predict the deformation of a single-lap joint in a tensile test with an average of error is 2.57%. This error can be reduced by a more accurate material model, more accurate measurements, more accurate testing comparison, and a more ideal testing setup.
- Alternative the geometry of the area in which the bonding process is performed, i.e., using SLJ, OSLJ and TSLJ has a profound impact on the stress concentrations forming at the adhesive joint and load carrying capacity of the joint.
- Comparison of load carrying capacities of joints bonded by stiff DP460 adhesive shows that OSLJ (Type-II b) and TSLJ (Type-III b) carried more 13% and 73% load than SLJ (Type-I b) did, respectively.
- Machining steps for the adhesively bonded joints (Type-III a) at the portions close to the edges of the overlap area decreased the peel stresses, formed at the edges of the overlap area, which are very effective in initiating damage and this decrease played a significant role in the increase of joint strength.
- Following to the data obtained from the experiments, for the joints bonded by flexible SBT9244 adhesive having the same bonding area, OSLJ (Type-II a) and TSLJ (Type-III a) carried more 11.5% and 56% load than SLJ (Type-I a) did, respectively.
- For Type-II and Type-III joints, both shear and peel stress distributions are homogeneous along the width (BC line), while for Type-I joint, the distributions took maximum values at the center along the width and minimum values at the edges and it is seen that great differences are evident between the stress values formed at the center and at the edges.

5.2 Future Work

There is an enormous area for further development. Future work can be carried out by changing the layer thickness and seeing how it influences the behavior of the structures.

1. In order to understand the affect varied material and geometric parameters have more deeply on the critical points' stresses, one varies more than one parameter at once, to understand how each parameter interacts with the other.
2. Suggested for extend the understanding of the failure behavior of adhesively bonded lap joints;
   - A more extensive test program can be designed to investigate the effect of composite stacking sequence in specimens with constant thickness.
   - A brittle adhesive material model can be created to simulate the cohesive crack in the adhesive bulk material.
3. Increase the accuracy of the experimental finite element model, one can do several things:
   - Develop a more accurate strain-dependent material model for both the adherend material and adhesive material.
   - Take steps to assure that the testing grips apply equal pressure to each clamped region and that they are as perfectly aligned as possible.
   - Ensure that all dimensional measurements are as accurate as possible, and that any machining that is needed is as accurate as possible, and that the gripped regions can be perfectly aligned vertically.

References

1. Grant LDR, Adams RD, da Silva LFM. Int J Adhes 2009; 29:405–13.
2. Patrick RL editor Treatise on adhesion and adhesives structural adhesives with emphasis on aerospace applications, vol.4.NewYork: Marcel Dekker, Inc.; 1976.
3. Sayman O, Arikan V, Dogan A, Soykok IF, Dogan T. Compos Part B 2013;54:409–14.
4. Gunes R, Apalak MK, Yildirim M, Ozkes I. Compos Struct 2010;92:1–17.
5. Uscinowicz R. Compos Part B 2013; 44:344–56.
6. Adams RD, Harris JA. Int J Adhes Adhes 1987; 7:69–80.
7. Zhao X, Adams R, da Silva LFM. J Adhes Sci Technol 2011; 25:837–56.
8. Akpinar S, Aydin MD, Ozel A. Appl Math Model 2013;37:10220–30.
9. Hoa, Suong V., Principles of the Manufacturing of Composite Materials, DEStech Publications, Inc., Pennsylvania, 2009.
10. S. Akpinar / Composites: Part B 67 (2014) 170–178.
11. https://en.wikipedia.org/wiki/Composite_material.
12. Palucka, T., & Bensaude-Vincent, B. (2002, October 19). Composites Overview.
13. Singh Ramesh, Composites Manufacturing, Indian Institute of Technology, Bombay.
14. Hart-Smith LJ (1973a, 1974) Analysis and design of advanced composite bonded joints. NASA Langley contract report NASA CR-2218, January 1973; reprinted, complete, August 1974.
15. Gosse JH, Christensen S (2001) Strain invariant failure criteria for polymers in composite materials. In: AIAA paper AIAA-2001-1184, presented to 42nd AIAA/ASME /ASCE/ AHS ASC structures, structural dynamics, and materials conference, Seattle, 16–19April 2001.
16. Hart-Smith LJ (1973b, 1973c, 1973d, 1973e) Analysis and design of advanced composite bonded joints. NASA Langley contract report NASA CR-2218.
17. Hart-Smith LJ (1973c, 1973d, 1973e) Analysis and design of advanced composite bonded joints. NASA Langley contract report NASA CR-2218.
18. Hart-Smith LJ (1982a) Design methodology for bonded bolted composite joints. USAF contract report AFWAL-TR-81-3154, 2 vols.
19. S.K.Panigrahi B.Pradhan Volume 29, Issue 2, March 2009, Pages 114-124.
20. Lembke A. Recovery-oriented policy and care systems in the UK and USA. Drug Alcohol Rev 2014; 33:13–18].
21. Thrall EW Jr, Shannon RW (eds) (1985) Adhesive bonding of aluminum alloys. Marcel Dekker, New York, pp 241–321
22. Experimental and Numerical Strength Analysis of Stepped Lap Adhesive Joints Subjected to Static Tensile Loading ISSN: 2278-0181, Vol. 6 Issue 09, September – 2017.

23. Heslehurst, R. B. (2013). Design and analysis of structural joints with composite materials. DEStech Publications, Inc.
24. L. F. M. da Silva and R. D. S. G. Campilho, Advances in Numerical Modeling of Adhesive Joints. 2012.
25. H. Khoramishad, A. D. Crocombe, K. B. Katnam, and I. A. Ashcroft, "Predicting fatigue damage in adhesively bonded joints using a cohesive zone model," Int. J. Fatigue, vol. 32, no. 7, pp. 1146–1158, 2010.
26. R. D. Adams, J. Comyn and W. C. Wake, Structural Adhesive Joints in Engineering, 2nd edn. Chapman & Hall, London (1997).
27. W. A. Lees, in: Adhesion-12, K. W. Allen (Ed.), pp. 141–158. Applied Science Publishers,London (1977).
28. T. R. Guess, R. E. Allred, and F. P. Gerstle, J. Testing Evaluation 5, 84–93 (1977).